



**Environmental
Science**
Processes & Impacts

**Wildland-Urban Interface Wildfire Increases Metal
Contributions to Stormwater Runoff in Paradise, California**

Journal:	<i>Environmental Science: Processes & Impacts</i>
Manuscript ID	EM-ART-07-2023-000298.R1
Article Type:	Paper

SCHOLARONE™
Manuscripts

Wildland-Urban Interface Wildfire Increases Metal Contributions to Stormwater Runoff in Paradise, California

Lauren J. Magliozzi ^a, Sandrine J. Matiasek ^b, Charles N. Alpers ^c, Julie Korak ^a, Diane McKnight ^a, Andrea L. Foster ^d, Joseph N. Ryan ^a, David A. Roth ^e, Peijia Ku ^f, Martin Tsz-Ki Tsui ^g, Alex T. Chow ^h, Jackson P. Webster ^{i*}

^a Environmental Engineering Program, University of Colorado Boulder;

^b Department of Earth and Environmental Sciences, California State University Chico;

^c California Water Science Center, United States Geological Survey, Sacramento, CA;

^d Geology, Minerals, Energy, and Geophysics Science Center, United States Geological Survey, Menlo Park, CA;

^e Water Mission Area, United States Geological Survey, Boulder, CO;

^f Environmental Sciences Division, Oak Ridge National Laboratory;

^g School of Life Sciences, State Key Laboratory of Agrobiotechnology, The Chinese University of Hong Kong;

^h Department of Forestry and Environmental Conservation, Clemson University;

ⁱ Department of Civil Engineering, California State University Chico

Keywords:

Wildfire, Water Quality, Stormflow, Contaminant Transport, Wildland-urban interface

Abstract

The 2018 Camp Fire was a large late-year (November) wildfire that produced an urban firestorm in the Town of Paradise, California, USA, and destroyed more than 18,000 structures. Runoff from burned wildland areas is known to contain ash, which can transport contaminants including metals into nearby watersheds. However, due to historically infrequent occurrences, the effect of wildland urban interface (WUI) fires, such as the Camp Fire, on surface water quality has not been well-characterized. Therefore, this study investigated the effects of widespread urban burning on surface water quality in major watersheds of the Camp Fire area. Between November 2018 and May 2019, 140 surface water samples were collected, including baseflow and stormflow, from burned and unburned watersheds with varying extent of urban development. Samples were analyzed for total and filter-passing metals, dissolved organic carbon, major anions, and total suspended solids. Ash and debris from the Camp Fire contributed metals to downstream watersheds via runoff throughout the storm season. Increases in concentration up to 200-fold were found for metals Cr, Cu, Ni, Pb, and Zn in burned watersheds compared to pre-fire values. Total

1 concentrations of Al, Cd, Cu, Pb, and Zn exceeded EPA aquatic habitat acute criteria by up to 16-
2
3 fold for up to five months after the fire. To assess possible transport mechanisms and
4
5 bioavailability, a subset of 18 samples was analyzed using four filters with nominal pore sizes
6
7 ranging from 0.22 to 1.2 μm to determine the particulate size distribution of metals. Trace and
8
9 major metals (Al, Ba, Co, Cr, Cu, Fe, Hg, Mn, Ni, Pb, and Zn) were found mostly associated with
10
11 larger grain sizes ($>0.45 \mu\text{m}$), and some metals (Al, Cr, Fe, and Pb) also included a substantial
12
13 colloidal phase (0.22 μm to 0.45 μm). This study suggests that fires in the wildland-urban interface
14
15 increase metal concentrations, mainly through particulate driven transport. The metals with largest
16
17 increases are likely from anthropogenic disaster materials, though biomass ash contributions are
18
19 also a major contributor to overall water quality. The increase in metals following WUI burning may
20
21 have adverse ecological impacts.
22
23
24
25
26

27 **Environmental Significance**

28
29
30 Wildfires that occur in forest and grassland landscapes are increasing in frequency and
31
32 intensity and are escalating the risk of burning at the wildland-urban interface (WUI). The effects of
33
34 wildfires in the WUI include loss of lives and livelihood, destruction of infrastructure, and long-term
35
36 impacts to ecosystems. Furthermore, fires that occur in the WUI may cause potential human or
37
38 ecological health issues through toxic metal contamination of surface waters in addition to smoke
39
40 inhalation risk.
41
42
43
44

45 **1. Introduction**

46
47 The Camp Fire was the deadliest, most destructive, and most expensive wildfire in California
48
49 history, and one of the costliest disasters in the world.¹ The fire killed 85 people and destroyed
50
51 18,804 structures across three communities (Paradise, Concow, and Magalia; Figure 1), resulting
52
53 in an estimated \$13 billion in losses and \$3 billion for cleanup.² Ignited by high-voltage power lines
54
55
56
57
58
59
60

1 on November 8, 2018, the fire started near Pulga in the Feather River Canyon, east of the Town of
2 Paradise and spread west due to high winds (80 km h⁻¹).² Due to the wind carrying embers that
3
4 sparked new ignitions downwind (i.e., firebrands), the Town of Paradise was consumed by fire
5
6 within three and a half hours, resulting in an urban firestorm.² In contrast to wildland fires, fires at
7
8 the wildland urban interface (WUI), such as the Camp Fire, combust anthropogenic materials that
9
10 may negatively impact surface water quality through runoff.
11
12
13
14
15

16 Fires in wildland areas (non-urban) are historically more common and have been the focus
17
18 of most research thus far. In vegetated watersheds, runoff after wildfires alters watershed
19
20 processes causing adverse impacts to surface water quality.³ Because of increased soil
21
22 hydrophobicity, rain mobilizes ash, soil, and charred materials, changing water chemistry (e.g., pH
23
24 and ionic composition) and increasing sediment transport, which in turn facilitates the mobilization
25
26 of metals associated with sediment.^{4,5,6,7} In wildland areas, mobilized metals can originate from a
27
28 variety of sources, such as burned biomass, disturbed underlying geology, and isolated mining and
29
30 manufacturing sites (historical or current).^{5,8,9,10} Elevated temperatures during combustion can alter
31
32 metal speciation or disrupt complexes with soil organic matter, often increasing mobility in surface
33
34 waters.^{8,11} Notably, some metals and metallic compounds pose acute adverse human and
35
36 ecosystem health effects.^{12,13}
37
38
39
40
41

42 In contrast, the water quality impacts of WUI fires have not been well-characterized because
43
44 of historically infrequent occurrence, but risk is expected to increase as the WUI expands due to
45
46 urban development.¹⁴ In urban fires, man-made fuels are combusted (e.g., structures, vehicles,
47
48 household products, and other infrastructure) creating “disaster materials”, which can include
49
50 asbestos fibers, man-made vitreous fibers (e.g., fiberglass insulation), metal-rich particles, and
51
52 particle-associated persistent organic pollutants.¹⁵ The extent of destruction and the variety of
53
54
55
56
57
58
59
60

1 anthropogenic source materials that could mobilize metals into the watershed, such as vehicles
2 (frames, batteries, wiring, tires), structures (residential, industrial, and commercial), and structure
3 contents (furniture, appliances, personal items) were widespread following the Camp Fire (Figure
4 2).
5
6
7
8
9

10
11 Storm runoff can mobilize metals from disaster materials. For example, runoff collected from
12 a simulated automobile fire conducted in the U.K. contained arsenic (As), barium (Ba), cadmium
13 (Cd), cobalt (Co), chromium (Cr), copper (Cu), mercury (Hg), nickel (Ni), lead (Pb), and zinc (Zn).¹⁶
14 In burned urban settings (London, U.K.) and on the urban fringe (California, USA), Cu, Pb, and Zn
15 concentrations in stormwater have been found 100 to 700-fold higher compared to unburned
16 areas.^{17,18,19,20} Additionally, WUI fires are, by definition, in close proximity to populated areas, and
17 the risk of elevated metals in stormwater runoff from these events is an emerging concern.^{17,18,21,22}
18
19
20
21
22
23
24
25
26
27

28 Although previous work has reported elevated metal concentrations in water from WUI fires,
29 metal speciation (e.g., phase partitioning) is not well-characterized despite its importance for
30 bioavailability and ecosystem health. At neutral pH, trace metals are commonly present in the
31 particulate or colloidal phase, sorbed to oxides of aluminum (Al), iron (Fe), or manganese (Mn), or
32 associated with humic substances.^{23,24} Speciation is important because dissolved (filter-passing)
33 trace metals are more readily assimilated by aquatic biota than particulate metals.^{25,26,27} While
34 dissolved organic matter (DOM) and trace metal mobilization may increase after a wildfire, toxicity
35 to biota may decrease if the bioavailability of trace metals decreases due to their complexation by
36 DOM.^{5,7,28} Therefore, it is important to understand both the quantity and speciation of metals
37 mobilized from WUI fires.
38
39
40
41
42
43
44
45
46
47
48
49
50

51 Because the large-scale urban destruction caused by the Camp Fire was a likely source of
52 anthropogenic contaminants, the goal of this study was to characterize metal concentrations in
53
54
55
56
57
58
59
60

1 surface water runoff from the burned area during storm events and baseflow conditions. We
2
3 evaluated water quality parameters, such as pH, specific conductivity, total suspended solids
4
5 (TSS), dissolved organic carbon (DOC), anions, and metals in the watersheds surrounding the
6
7 Town of Paradise after the Camp Fire. We hypothesized that runoff would increase metal
8
9 concentrations in surface waters, and that increases would be greater in watersheds with a greater
10
11 extent of urban destruction. Therefore, the objective of this study was to characterize the effects of
12
13 burned anthropogenic materials, such as vehicles and structures, on stormwater metal
14
15 concentrations.
16
17
18
19
20

21 **2. Methods**

22 **2.1. Site and Watershed Descriptions**

23
24
25
26 Paradise (population 26,800 pre-fire) is a town located on the western slope of the Sierra
27
28 Nevada and the southern Cascade Range in California (Figure 1). The town is located on
29
30 moderately-sloping to level ridges surrounded by steep canyons carved by creeks that flow to the
31
32 Sacramento Valley to the southwest and Lake Oroville to the southeast. The landscape is
33
34 dominated by oak woodlands and grasslands southwest of town and Sierran mixed conifers at
35
36 higher elevations along the northeast watershed border.
37
38
39
40

41 The dominant soil in the Paradise ridge is the Paradiso soil series, a loam formed on clayey
42
43 residuum weathered from volcanic rock (Alfisol order, Xeralfs suborder of the USDA soil
44
45 classification).²⁹ Clay in the surface horizon (top 10 cm) is primarily kaolinite ($\text{Al}_2\text{Si}_2\text{O}_5(\text{OH})_4$), a
46
47 highly weathered 1:1 non-expansive aluminosilicate clay with low cation exchange capacity, and
48
49 therefore limited potential for ion exchange with metals.
50
51
52
53
54
55
56
57
58
59
60

1 Four major watersheds near the Town of Paradise were sampled (Table 1): Big Chico
2 Creek, Butte Creek, Clear Creek, and Dry Creek (coordinates in Table S1), which represent a
3 variety of burn conditions and land uses. Big Chico Creek is an unburned reference watershed.
4 Butte Creek is a semi-urban and forested watershed that was partially burned. Clear Creek and Dry
5 Creek were both severely burned, and Clear Creek has more urban development than Dry Creek.
6 In this context, urban refers to the areas of highest population density in this region, which do not
7 meet the criteria for large cities.

8 Watershed characteristics, including elevation, land use, area, and structure damage
9 assessment, were determined using ArcGIS (Esri, USA). Watershed area was defined as the
10 contributing area for the sampling location. A variety of sources were used to analyze land use
11 characteristics, number of destroyed structures, soil and bedrock geology, and historical mining
12 activities.^{30,31,32,33} There was mining in each watershed to varying degrees. Due to the presence of
13 many small mines that were not major producers, the area of mine tailings was assumed to be a
14 better indicator of potential water quality effects than the number of mines.

15 Discharge measurements were only available at the USGS Butte Creek stream gage station
16 (USGS 11390000), which was used to synchronize sample collection with peak stormflows for all
17 watersheds (Figure 3). This gage is located upstream of the western most sample location in Butte
18 Creek (Figure 1). During the 2018-2019 water year, precipitation in Paradise, CA was
19 approximately 1.3 times greater than the yearly average from 2010-2020.³⁴ Flows for a two-year
20 recurrence interval were estimated with StreamStats (USGS, v4.1.1) providing the reader with a
21 sense of relative stream sizes across watersheds.³⁵

22 *2.1.1. Big Chico Creek*

1 Big Chico Creek is an unburned watershed sampled for comparison to the burned
2
3 watersheds. No gaging station monitored discharge on a continuous basis during the 2018-19
4
5 storm season, but historical flow rates are between $0.6 \text{ m}^3 \text{ s}^{-1}$ (summer baseflow) and $170 \text{ m}^3 \text{ s}^{-1}$
6
7 (winter stormflow).³⁶ The watershed has lower urban land use area (1%) and a higher percentage
8
9 of forested area (69%) compared to the other watersheds (Table 1). The watershed originates at
10
11 1829 m elevation and extends west for about 43 km to the Sacramento River. The upper
12
13 watershed is characterized by Cascade Range basalt at high elevations and lava and mud flows
14
15 from the extinct Mount Yana volcanic complex at lower elevations.³⁷ Vegetation transitions from
16
17 Ponderosa pine and mixed fir at high elevations to California mixed conifer and oak grasslands at
18
19 lower elevations. There have been a few small fires in the watershed at low elevations, but no
20
21 major fire events in the past decade. There are two historic, closed gold mines upstream, but their
22
23 combined area is small ($< 1 \text{ km}^2$).³⁸
24
25
26
27
28

29 Samples were collected at multiple locations along Big Chico Creek. Sampling occurred at
30
31 the Big Chico Creek Ecological Reserve (15 km upstream of the city of Chico) with an autosampler
32
33 when possible. Access was limited during large storms, and, on those occasions, grab samples
34
35 were collected lower in the watershed, east of and 3 km upstream from the City of Chico.
36
37
38

39 *2.1.2. Butte Creek*

40 The Butte Creek watershed has similar characteristics to the Big Chico Creek watershed.
41
42 The creeks originate within 2 km of one another and generally flow within a few miles of each other.
43
44 Butte Creek also has low urban land use (4%) and high forested area (69%) (Table 1). In contrast
45
46 to Big Chico Creek watershed, 16% of Butte Creek watershed was burned, and the watershed
47
48 contains the highest number of total structures burned. Mine tailings impact about 1.2 km^2 of the
49
50 watershed ($< 1\%$), with inactive gold mines and a small number of inactive chromium mines.³⁸
51
52
53
54
55
56
57
58
59
60

1 Discharge in Butte Creek ranged from late fall baseflow of $\sim 2 \text{ m}^3 \text{ s}^{-1}$ at the time of the Camp Fire to
2 storm flows as high as $230 \text{ m}^3 \text{ s}^{-1}$ in late February storms (Figure 3). Like the observed maximum
3 flows, the estimated two-year return interval stormflow is $212 \text{ m}^3 \text{ s}^{-1}$. This similarity justifies the use
4 of two-year return intervals to provide comparative estimates of stormflow discharges in streams
5 that did not have stream flow measurements.
6
7
8
9
10
11
12

13 Grab samples were collected at the USGS gaging station located in the lower reach of Butte
14 Creek Canyon (Figure 1). When deploying an autosampler, samples were collected at the Butte
15 Creek Ecological Preserve (BCEP) for increased security. These locations are 1.4 km from each
16 other with no major water inputs or withdrawals between locations.
17
18
19
20
21
22

23 Little Butte Creek Trailer Park (Figure 2b and Figure 2c) was located along Little Butte
24 Creek, a tributary of the Butte Creek watershed. All trailers and many vehicles in the park were
25 destroyed by the fire. Storm runoff was collected from an intermittent stream draining the trailer
26 park in January 2019 prior to site cleanup. This location represents a burned, urban end-member
27 with direct runoff from burned anthropogenic materials.
28
29
30
31
32
33
34
35

36 2.1.3. *Clear Creek*

37 Clear Creek originates within the Town of Paradise amid residential and light commercial
38 development. The watershed is defined by the highest percentage of total burned area (78%) and
39 urban land use area (18%) compared to the other watersheds (Table 1). The two-year return
40 interval stormflow is estimated at $20 \text{ m}^3 \text{ s}^{-1}$. Sampling was conducted west of Highway 191 at
41 Durham Pentz Road, about 14.5 km downstream of the Town of Paradise, which was initially the
42 closest accessible location to the burned area due to prolonged evacuation orders (Figure 1). No
43 known mines are present in this watershed.
44
45
46
47
48
49
50
51
52
53
54
55
56
57
58
59
60

2.1.4. *Dry Creek*

Dry Creek also originates in the Town of Paradise. The Dry Creek watershed was 45% burned (by area) by the Camp Fire (Table 1). Dry Creek has a higher percentage of total percent forested land (33%) than total percent urban land (9%). This watershed has inactive gold and manganese mines attributing to both the largest mining-impacted area on both an absolute (total area) and relative (percent area) basis. Downstream of the fire perimeter, Dry Creek receives drainage from the Cherokee mine: a large, inactive hydraulic gold mining operation, which contributes sediment to the creek.³⁹ The two-year return interval stormflow is estimated to be $37 \text{ m}^3 \text{ s}^{-1}$. Dry Creek was sampled about 17 km downstream (south) of the edge of the Town of Paradise.

2.1.5. *Paul Byrne Aquatic Park*

Grab samples were collected from an unnamed, intermittent first-order stream at Paul Byrne Aquatic Park near the south edge of the Paradise ridge, which is in the Little Dry Creek watershed. This sampling location was dominated by direct stormwater runoff during rain events. Since the Town of Paradise spans several watersheds, this sampling location represents a burned, urban end-member capturing typical anthropogenic inputs to Clear Creek from within the Town of Paradise. Samples were collected when access permitted. The two-year return interval stormflow estimate is $2 \text{ m}^3 \text{ s}^{-1}$.

2.2. **Sampling Methods**

Water samples were collected during nine storm events between November 2018 and May 2019 targeting different flow regimes including baseflow, peak storm flow, and rising and falling limbs of the stormflow hydrograph (Figure 3). A total of 140 grab samples were collected in new, high- or low-density polyethylene bottles that were tested for trace metal contamination using lab and field blanks. Sampling followed best practices, using nitrile-gloved hands, triple rinsing bottles

1 with sample water prior to collection, sealing, and storing on ice until returning to the California
2 State University Chico laboratory. During intensive storm sampling efforts, automatic samplers
3 (Teledyne ISCO 6712) collected water in reusable, 1-L acid-washed (10% nitric acid)
4 polypropylene bottles stored on ice. Bottles were retrieved within 24 h of sampling. In the
5 laboratory, samples were stored at 4 °C until filtration and further processing for analyses within 48
6 h.

16 **2.3. Water Quality Measurements**

18 Prior to filtration, pH and specific conductivity were measured in well-mixed water samples
19 at room temperature with an Oakton PCSTestr 35 handheld meter with integrated pH and specific
20 conductivity probes, calibrated daily. Total suspended solids (TSS) were quantified by filtering a
21 known volume of water sample (0.45 µm). Dissolved organic carbon (DOC) was measured using a
22 high-temperature catalytic oxidation method (TOC-L, Shimadzu). Sulfate and nitrate were
23 measured by ion chromatography (Integrion, Dionex). Elemental analysis was conducted using
24 inductively-coupled plasma mass spectrometry (ICP-MS) (7900, Agilent). Elemental analysis
25 included Al (aluminum), As (arsenic), Ba (barium), Ca (calcium), Cd (cadmium), Co (cobalt), Cr
26 (chromium), Fe (iron), K (potassium), Mg (magnesium), Mn (manganese), Na (sodium), Ni (nickel),
27 Pb (lead), Tl (thallium), Se (selenium), U (uranium), V (vanadium), and Zn (zinc). For alkali and
28 alkaline earth elements, Ca, K, Mg, and Na are commonly observed at ppm concentrations and are
29 collectively referred to as major cations, which excludes Ba. Important for the EPA aquatic life
30 criteria, hardness (as mg L⁻¹ CaCO₃) was calculated using Equation S1. Capturing differences in
31 relative concentrations, Al, Fe, and Mn are described as major metals and remaining elements are
32 described as trace metals. Total concentrations refer to concentrations measured in unfiltered
33 samples. For metal, filter-passing concentrations were measured in the filtrate of a 0.45-µm

1 cellulose nitrate filter. Total mercury (THg) was quantified on a subset of 54 samples using cold-
2 vapor atomic fluorescence spectrometer (Model III, Brooks and Rand). Additionally, metals analysis
3
4 by size fractionation within the colloidal range 0.22- μm to 1.2- μm was assessed. The grain size
5
6 analysis methods and tabulated results are described in an associated USGS Data release.⁴⁰
7
8 Additional details for each analytical method are provided in the supporting information.
9
10
11
12

13 **2.4. Statistical Methods**

14
15
16 Statistical analyses were performed with R Statistical Software (v4.2.1);⁴¹ specific functions
17 are listed in parentheses. The Shapiro test (`shapiro.test()`) indicated that the datasets were non-
18 normal. We compared concentrations pre- and post-fire using the Wilcoxon U test (`wilcox.test()`)
19 followed by the pairwise Wilcoxon U test (`pairwise.wilcox.test()`) if there were statistically significant
20 differences. Correlations between water quality parameters were assessed using Spearman's rank
21 correlations (`ggpairs()`, GGally R package v2.1.2).⁴² Principal component analysis (PCA) analyzed
22 water quality parameters in reduced space (`prcomp()`, stats R package v4.2.1).⁴¹ Data was
23 standardized prior to analysis. A redundancy analysis (RDA) assessed relationships between water
24 quality and watershed characteristics, structure destruction, TSS, and flow (`rda()`, vegan R package
25 v2.6.2).⁴³ Explanatory and response variables were standardized prior to analysis.
26
27
28
29
30
31
32
33
34
35
36
37
38
39

40 **3. Results**

41 **3.1. Water Quality Comparisons**

42
43
44 Aggregate water quality parameters were compared between watersheds to assess
45 systematic trends, independent of temporal hydrology. The median concentrations for DOC,
46 sulfate, and nitrate were higher in Clear Creek and Dry Creek watersheds, which had the highest
47 number of destroyed structures per urban area (number of destroyed structures divided by area of
48
49
50
51
52
53
54
55
56
57
58
59
60

1 urban land use in each watershed), compared to the unburned reference watershed. For example,
2 the median DOC concentrations in Dry Creek and Clear Creek (4.5 mg L^{-1} and 4.6 mg L^{-1} ,
3 respectively) were twice as high as the median DOC concentrations in Butte Creek and Big Chico
4 Creek (1.8 mg L^{-1} and 2.1 mg L^{-1} respectively, Table S5). Similarly, concentrations of sulfate,
5 nitrate, TSS, and hardness (Figure 4a) were statistically higher in Clear Creek and Dry Creek
6 (Wilcoxon U test, $p < 0.05$, Table S9). In all watersheds, pH values were circumneutral and ranged
7 from 7.1 to 8.3 (Table S5). Like DOC, sulfate, and nitrate, total concentrations of many metals (i.e.,
8 Ba, Co, Cu, Pb, Ni, Mn, and Zn) were significantly greater (Wilcoxon U, $p < 0.05$, Table S9) in
9 burned watersheds compared to the unburned Big Chico Creek reference watershed (Figure 4b,
10 Table S11). However, there were two exceptions. For Al and Cr, there was no statistically
11 significant difference between Clear Creek and the unburned Big Chico Creek. In Dry Creek, the
12 watershed with the greatest increase in median concentrations relative to unburned Big Chico
13 Creek, Co median concentrations increased 36-fold, followed by Cu, Fe, Mn, Ni, and Pb (36- to 22-
14 fold). Ba, Cr, Ni, and Zn median concentrations were 7-to 17-fold greater in Dry Creek compared to
15 the reference watershed.

16
17
18
19
20
21
22
23
24
25
26
27
28
29
30
31
32
33
34
35
36
37 Little Butte Creek Trailer Park and Paul Byrne Aquatic Park (burned, urban end-members)
38 represent sites with the greatest burned, urban impact as there was less dilution compared to the
39 mainstem sampling locations. At these sites, total concentrations of metals were also higher than
40 the unburned watershed and burned watersheds with more dilution. The maximum concentrations
41 of Cu ($25 \text{ } \mu\text{g L}^{-1}$), Pb ($4.9 - 6.5 \text{ } \mu\text{g L}^{-1}$), and Zn ($1100 \text{ } \mu\text{g L}^{-1}$) exceeded the maximum
42 concentrations measured in mainstem sampling locations. At the Aquatic Park site, the median
43 concentration of total Pb was higher than the other mainstem locations ($4.9 \text{ } \mu\text{g L}^{-1}$). The maximum
44 total Zn concentration at the Aquatic Park ($256 \text{ } \mu\text{g L}^{-1}$) was also high compared to the mainstem
45
46
47
48
49
50
51
52
53
54
55
56
57
58
59
60

1 locations, but the highest concentration was observed at the Little Butte Creek Trailer Park (1,079
2 $\mu\text{g L}^{-1}$, Table S7).
3
4

5
6 Throughout the 2018/2019 water year, the highest concentrations of total and filter-passing
7 metals were observed near or directly after the hydrograph flow peaks (Figures S1- S3). Early
8 precipitation events (November –December 2018) produced lower flows than later precipitation
9 events in January–March 2019 (Figure 3). However, the early season concentrations of many
10 alkaline and alkaline earth elements were elevated beyond the later season storm flow
11 concentrations (Figures S1-S7). Similarly, some of the highest observed Al, Cu, Pb, and Zn
12 concentrations were in the fire-impacted watersheds in December 2018–January 2019. Across
13 nearly all watersheds and flow regimes, total Hg concentrations were near background levels (1–5
14 ng L^{-1} , Table S6).⁴⁴
15
16
17
18
19
20
21
22
23
24
25
26
27

28 **3.2. Size-Fraction Analysis of Trace and Major Metals**

29
30 Total and filter-passing metal concentrations were compared to assess the predominant
31 phase (i.e., particulate vs. dissolved) of each metal. After calculating the percent particulate for
32 each sample, the median value for each element was used to group elements according to their
33 predominant phase. Oxide-forming elements, including Al, Fe, Mn, were predominantly measured
34 in the particulate phase (Figure S8 and Figure S9). Similarly, most trace metals were
35 predominantly found in the particulate fraction, except for Ba, Cu, and Ni that exhibited a fairly
36 uniform distribution between particulate and filter-passing fractions. Alkaline and alkaline-earth
37 elements (Ca, K, Na, and Mg) were predominantly filter-passing.
38
39
40
41
42
43
44
45
46
47
48
49

50 Filter-passing metal concentrations ($< 0.45 \mu\text{m}$) were generally higher in burned watersheds
51 when compared to the unburned Big Chico Creek watershed, but differences were not statistically
52 significant ($p > 0.05$) in most cases (Figure 5). The exception was Butte Creek, where
53
54
55
56
57
58
59
60

1 concentrations of filter-passing Co were statistically greater than in the reference watershed ($p =$
2
3
4 1.5×10^{-3}).

5
6 The size fractionation analysis (filter sizes 0.22 μm , 0.45 μm , 0.8 μm , and 1.2 μm) revealed
7
8 that four elements (i.e., Al, Cr, Fe, and Pb) had statistically higher concentrations (Wilcoxon U, $p <$
9
10 0.05, Table S10) in the 1.2 μm filtrate compared to the 0.22 μm filtrate, suggesting colloidal
11
12 association (Figure 6). Al was the only metal with statistically different concentrations between the
13
14 0.22 μm and 0.45 μm filter sizes, revealing a slightly wider distribution of colloidal sizes. Comparing
15
16 median concentrations between filter-size cutoffs to the median total metal concentration informs
17
18 the proportion of a given metal associated with intermediate colloidal sizes. For the elements with
19
20 statistically significant differences, the median percentage associated with the 0.22–1.2 μm fraction
21
22 was 65.6% for Al, 14.3% for Cr, 62.1% for Fe, and 68.6% for Pb. In contrast, no statistically
23
24 significant difference between filter size cutoffs was observed for Co, Cu, Mn, or Ni, hence most of
25
26 these elements were either dissolved or associated with the smallest colloidal size fractions.
27
28
29
30
31

32 To summarize, most trace metals were present predominantly as particulates (Figure S9),
33
34 and the only trace metals that did not exhibit a dominant particulate form were Ba, Cu, and Ni.
35
36 These elements were broadly distributed across phases (Figures S8 and S9) and Cu did not exhibit
37
38 an appreciable colloidal fraction (Figure 6). Cr and Pb were predominantly (67% or more) found in
39
40 the particulate fraction using a 0.45 μm filter cutoff (Figure S9) and these elements also had
41
42 measurable colloidal fractions in half of the samples (Figure 6).
43
44
45
46

47 **3.3. Comparison to Historical Data**

48
49 In contrast to many disaster response studies, some historical data exist for hardness in the
50
51 four burned watersheds and for select trace metals in two burned watersheds.³⁹ Total median
52
53 concentrations of Cr, Cu, Ni, Pb, and Zn significantly increased in Clear Creek and Dry Creek after
54
55
56
57
58
59
60

1 the Camp Fire compared to pre-fire concentrations (Figure 7, Table S12). The greatest increase
2 was observed for total Zn in both Dry Creek (200-fold) and Clear Creek (22-fold). For Cr and Pb,
3 greater increases were observed in Dry Creek (30- and 22-fold, respectively) compared to Clear
4 Creek (6-fold for both). Cu and Ni concentrations were 3- to 8-fold higher in samples collected after
5 the fire. The pre-fire data were collected through monthly storm sampling from November 2003 to
6 December 2004 in Clear Creek and Dry Creek. Comparing the 2003-2004 and 2018-2019
7 hydrographs in Butte Creek revealed that storm flow patterns were similar throughout the two years
8 (Figure S25).³⁴

9
10
11
12
13
14
15
16
17
18
19
20
21 Comparing annual averages, no statistically significant differences in hardness were found
22 between pre- and post-fire divalent cations in all four watersheds, further supporting the
23 comparability of pre- and post-fire datasets. However, the time-series graphs with data from 2003-
24 2004 show consistent hardness concentrations (50-60 mg L⁻¹ as CaCO₃) throughout the year in
25 Dry Creek and Clear Creek (Figures S4-S7). After the fire, hardness was >90 mg L⁻¹ as CaCO₃ and
26 systematically decreased during the first two months after the fire.

34 35 **3.4. Implications for Aquatic Health**

36
37
38 Metal concentrations were compared to both the EPA acute and chronic aquatic life criteria
39 to assess potential impact on ecosystem health.⁴⁵ Only samples with exceedances are discussed
40 in this section (Table 2, Table S13).

41
42
43
44
45 The EPA acute aquatic life criteria were exceeded during many sampling events for total Al,
46 Cu, and Zn (Table 2). Total Al exceeded criteria in 51 of 140 samples (36%). Cu exceeded life
47 criteria in 77 cases, with 50 cases for filter-passing samples and 27 cases for total samples. The Zn
48 limit was exceeded in 52 cases, with three cases for filter-passing samples and 49 cases for total
49 samples. For all three elements, the highest number of exceedances occurred in Butte Creek
50
51
52
53
54
55
56
57
58
59
60

1 followed by Clear Creek and Dry Creek. Butte Creek had the highest exceedance concentration for
2
3 both Al at 21-times the limit (February 14, 2019) and Cd at 3.5-times the limit (January 11, 2019).
4
5 The unburned reference watershed, Big Chico Creek, had fewer exceedances for all elements than
6
7 the fire-impacted watersheds.
8
9

10
11 Not only did samples from the urban end-member sites (Paul Byrne Aquatic Park and Little
12
13 Butte Creek Trailer Park) exceed standards, but the highest concentrations for Cu, Pb, and Zn,
14
15 were observed at these sites. Samples from Paul Byrne Aquatic Park had the highest acute criteria
16
17 exceedance concentrations for Cu at 8.4-times the limit, and Pb at 1.5-times the limit, both on May
18
19 15, 2019 during a summer storm event. The highest exceedance concentration for Zn was
20
21 detected at Little Butte Creek Trailer Park on December 18, 2018, at 11-times greater than the
22
23 acute limit.
24
25

26
27 The EPA chronic aquatic life criteria concentration limit was exceeded for Al (121 cases), Cd
28
29 (1), Cu (101), Ni (10), Pb (51), and Zn (50), with the highest exceedance noted for Al (16-fold in
30
31 Butte Creek, Table 2).
32
33
34
35

36 **3.5. Statistical Relationships**

37 *3.5.1. Spearman's Rank Correlations*

38
39 To assess potential sources and transport mechanisms of contaminants, correlations
40
41 between water quality characteristics were initially assessed using Spearman's rank correlations.
42
43 Correlations were first calculated with data aggregated across all watersheds (Figure S10) and
44
45 then divided into two subsets to assess if any correlations were unique to burned (Figure S11) or
46
47 unburned (Figure S12) watersheds. Correlations for each subset were also calculated for filter-
48
49
50
51
52
53
54
55
56
57
58
59
60

1 passing (Figures S13-S15) and particulate (Figures S16-S18) trace metal concentrations. Heat
2 maps in Figures S10-S18 only report correlation coefficients (ρ) for $p < 0.05$.
3
4

5
6 For total metal concentrations in all watersheds, there were strong positive correlations
7 between all combinations of Al, Ba, Cu, Co, Cr, Fe, Mn, Pb, and TSS ($\rho > 0.42$, Figure S10). When
8 comparing burned and unburned watersheds (Figures S11 and S12), only Zn showed statistically
9 significant correlations with these same trace elements in burned watersheds and not in the
10 reference watershed Big Chico Creek. Additionally, in the unburned reference watershed, DOC
11 was positively correlated ($\rho = 0.42$ to 0.65) with TSS, nitrate, and several trace metals (i.e., Al Co,
12 Cu, Fe, Mn). DOC was not correlated with TSS in burned watersheds. In the burned watersheds,
13 nitrate and sulfate were correlated with nearly all constituents.
14
15
16
17
18
19
20
21
22
23
24
25

26 Considering only filter-passing metals, correlations were calculated for trace metals and
27 other water quality parameters (Figures S13-S15). In general, there were more correlations
28 between filter-passing metals and other water quality parameters in the burned watersheds
29 compared to the unburned watershed. Filter-passing Cu was strongly correlated with Pb in both
30 watershed subsets ($\rho = 0.81$ to 0.89). Between all the trace elements, the number of pairs with
31 significant positive correlations was higher across burned watersheds (31) compared to the
32 unburned watershed (15), where one pair was inversely correlated (Zn vs. Fe, $\rho = -0.38$).
33
34
35
36
37
38
39
40
41
42

43 For the particulate fraction, correlations were explored for trace elements and other water
44 quality parameters (Figures S16-S18). In burned watersheds, all trace metals were positively
45 correlated with one another and with TSS ($\rho = 0.44$ to 0.96), except for Cu and Zn that had no
46 significant correlation with each other. In the unburned watershed, many of the same pairs were
47 positively correlated except for Ba, Cu, and Zn.
48
49
50
51
52
53
54
55
56
57
58
59
60

3.5.2. *Principal Component Analysis (PCA)*

Because Spearman correlations are limited to paired comparisons, PCA was used to investigate correlations between groups of water quality parameters simultaneously. PCA was performed using total trace metal concentrations as descriptors for each watershed individually (Figure S19) and all watersheds collectively (Figure S20). PCA was also performed for all watersheds with water quality parameters (i.e., ionic composition, DOC, TSS etc.) as descriptors in combination with total (Figure 8), filter-passing (Figure S21), and particulate (Figure S22) trace metal concentrations. For each descriptor, the vector length and direction (rotation) describe the relationship between descriptor and principal components; rotation values for each PCA are reported in Table S14. The angle between vectors communicates the correlation between descriptors, with a more acute angle representing a higher association.

Correlations within the most abundant, oxide-forming elements (i.e., Al, Fe, Mn) vs. within other trace elements were compared (Figures S10-S12, S16-S18) because statistical correlations may be indicators of physical transport mechanisms (e.g., adsorption onto oxides). Correlations between oxide-forming elements were watershed specific. For example, Al was strongly correlated with Fe ($<5^\circ$ between vectors) in all watersheds (burned and reference) except for Dry Creek (78°), and Al was only strongly correlated with Mn in Butte Creek (9°). Fe and Mn were not significantly correlated ($>10^\circ$) in any watershed. Correlations between oxide-forming elements and other trace elements were also watershed specific. Mn was strongly correlated ($<10^\circ$) with Co and Zn in one burned watershed (Clear Creek) and with Ba, Cu, and Pb in the unburned watershed (Big Chico Creek). In burned watersheds, Al was strongly correlated ($<10^\circ$) to Cu and Pb in Clear Creek, and Cr and Ni in Dry Creek, but Fe was correlated with Cu (3°) and Pb (5°) in Clear Creek and with Ba in Dry Creek (8°).

1 PCAs were also performed to examine the relationships among the whole suite of chemical
2
3 parameters (i.e., trace metals, major cations, pH, DOC, nitrate, and sulfate) across all watersheds
4
5 for total (Figure 8), filter-passing (Figure S21), and particulate (Figure S22) metal concentrations.
6
7 Describing 65% of the variation, the total metal PCA revealed two major descriptor groupings
8
9 where all metals (Group A) were almost orthogonal to the other water quality parameters (Group B)
10
11 including Ca, K, Mg, Na, DOC, nitrate, sulfate, and pH (Figure 8). Because trace elements were
12
13 predominantly in the particulate form (Figure S9), these groupings effectively divided descriptors by
14
15 phase, with Group A consisting of particulate constituents and Group B representing constituents
16
17 more likely to be truly dissolved. Vectors for Group A were oriented in the negative PC1 direction,
18
19 with all vectors pointed away from unburned reference watershed Big Chico Creek. Angles
20
21 between some pairs of Group A vectors showed closer associations with one another compared to
22
23 Group B. For example, several pairs of elements had nearly overlapped vectors, which was not
24
25 observed in Group B.
26
27
28
29
30
31

32 Although total metal concentration PCAs described >65% of the variance, one limitation of
33
34 performing PCA with total metal concentrations is that the analysis does not differentiate between
35
36 filter-passing and particulate concentrations. However, the filter-passing metal PCA explained only
37
38 53% of the variance (Figure S21), indicating that more components or variables were needed to
39
40 model the filter-passing metal dataset, which was not interpreted further. Because PCA requires a
41
42 detected concentration for every element, PCA with particulate metals only included a subset of
43
44 elements to retain the greatest number of samples in the analysis. The threshold to include an
45
46 element was that the median value for percent particulate was at least 50% (Figures S8- S9) to
47
48 minimize excluding samples due to non-detects. The particulate metal PCA (Figure S22) explained
49
50 84% of variance and showed similar vector relationships to the total concentration PCA (Figure 8).
51
52
53
54
55
56
57
58
59
60

1 All vectors were anti-correlated with (pointing away from) the unburned reference watershed (Big
2 Chico Creek). Based on the low percentages of variance explained in several PCAs, and
3
4 watershed-specific relationships between PCAs, a statistical analysis that uses explanatory
5
6 variables, such as RDA, is needed to better model water quality (Figure S22).
7
8
9

10 11 3.5.3. Redundancy Analysis (RDA) 12

13
14 An RDA model revealed that water quality variation (96%) could be modeled by a
15
16 combination of four explanatory variables: percent of urban land use in each watershed (urban
17 area (%)), number of destroyed structures in each watershed, TSS concentration in each sample,
18
19 and flow as measured in Butte Creek. Flow was only measured at one location, varying temporally
20
21 but not spatially between watersheds in this RDA model. The number of destroyed structures and
22
23 urban area (%) varied spatially by watershed but not temporally. TSS varied both temporally and
24
25 spatially for each unique sample. The other water quality parameters were used as dependent
26
27 variables, including total concentrations of trace metals, major cations, major anions, and DOC
28
29 (Figure 9). The supporting information includes RDA models for filter-passing (Figure S23) and
30
31 particulate trace metal concentrations (Figure S24).
32
33
34
35
36

37
38 In the RDA analysis, the multidimensional data were reduced to two main axes that
39
40 represent linear combinations of the explanatory variables. The RDA results provided the
41
42 coefficients for each explanatory variable in these two axes (Figure 9), described in Equation 1 and
43
44 Equation 2. For example, RDA1 increased with flow, TSS, and destroyed structures, and
45
46 decreased with urban area (%). Comparatively, RDA2 was more sensitive to urban areas (%) (i.e.,
47
48 larger coefficient), less sensitive to destroyed structures, and insensitive to flow. Because the first
49
50 two axes together explained 96% of variance, additional axes were not interpreted. Each point
51
52
53
54
55
56
57
58
59
60

1 represents a discrete sample projected onto RDA1 and RDA2 with the shaded areas in Figure 9,
 2
 3
 4 outlining each watershed.

$$\begin{aligned}
 \text{RDA1} = & (-0.282 \times \text{Urban area (\%)}) + (0.343 \times \text{Destroyed Structures}) \\
 & + (0.607 \times \text{TSS}) + (0.878 \times \text{Flow})
 \end{aligned}
 \tag{Eqn. 1}$$

$$\begin{aligned}
 \text{RDA2} = & (0.857 \times \text{Urban area (\%)}) + (0.165 \times \text{Destroyed Structure}) \\
 & + (0.652 \times \text{TSS}) + (-0.078 \times \text{Flow})
 \end{aligned}
 \tag{Eqn. 2}$$

18 Like PCA, the RDA vectors for the water quality parameters are divided into two groups,
 19 separating the trace metals (Group A) from Ca, K, Mg, Na, DOC, nitrate, sulfate, and pH (Group B).
 20
 21 The central tendency of each group was approximately orthogonal (e.g., Ca vs. Al), similar to
 22
 23 Figure 8 for PCA. However, compared to PCA, the RDA identified some key differences. In PCA,
 24
 25 Mn and Ba were strongly correlated (Figure 8). In the RDA, the correlation between Mn and Ba
 26
 27 was weaker, but the correlation between Mn and nitrate was stronger. Lastly, the RDA affirmed
 28
 29 strong correlations ($<3^\circ$) between trace metals and oxide-forming metals, including Cr-Cu, Fe-Cu,
 30
 31 Fe-Cr, Cr-Ni, and Al-Ni.

36
 37 Comparing vectors to the independent variable markers shows the relative association
 38
 39 between water quality and the different spatial and temporal explanatory variables (Figure 9). In the
 40
 41 reduced space of the RDA, Group A metal vectors aligned most with the number of destroyed
 42
 43 structures and TSS. In contrast, three of the Group B constituents (sulfate, nitrate, and DOC)
 44
 45 aligned with urban area (%). Na and K were differentiated from the other Group B constituents and
 46
 47 anticorrelated with flow. Figure 9 also showed that increases in flow corresponded to increases in
 48
 49 trace metal concentrations but not increases for major ions or DOC.
 50
 51
 52
 53
 54
 55
 56
 57
 58
 59
 60

1 RDA was also performed for filter-passing concentrations using only three explanatory
2 variables: urban area (%), number of destroyed structures, and flow. The RDA for filter-passing
3 concentrations explained 99% of the variance (Figure S23, Equations S2 and S3). Most of the
4 variance was described by RDA1 (92%), where urban area (%) had the only positive coefficient
5 whereas flow had an almost equal and opposite coefficient. In contrast to Figure 9, the filter-
6 passing analysis suggested that most trace elements and dissolved Group B constituents aligned
7 with urban area (%), not destroyed structures. Found predominantly in the filter-passing fraction,
8 Cu was most closely aligned with the number of destroyed structures, as also seen in Figure 9.
9 Although predominantly particulate, Zn was observed at appreciable filter-passing concentrations
10 (1-10 $\mu\text{g L}^{-1}$) and its vector nearly bisected the two variables associated with urban wildfire (urban
11 area (%) and destroyed structures). Other close associations in the filter-passing fraction included
12 Pb and Co and Ba and sulfate. All concentrations were anti-correlated with flow along RDA1. With
13 respect to RDA1 and RD2, all water quality vectors were oriented away from the unburned
14 reference watershed Big Chico Creek.

15 Lastly, an RDA was created for particulate concentrations using the same metals as the
16 particulate PCA (Figure S24) with the same explanatory variables as Figure 9. Over 99% of the
17 variance was explained by RDA1, which is heavily weighted by TSS (Equations S4 and S5). Only
18 38 samples had complete data sets (i.e., detects for each element) to perform this RDA.

4. Discussion

4.1. Metal Controls and Sources

19 The primary hypothesis – that widespread urban burning would increase concentrations of
20 metals in storm runoff – was supported by the analysis. Metal concentrations were consistently
21 elevated in burned watersheds compared to the unburned reference watershed (Figure 4).

1 Compared to available historical data, total concentrations of Cr, Cu, Ni, Pb, and Zn were up to
2
3 200-fold higher in Dry and Clear Creeks after the fire (Figure 7). Previous studies reported that WUI
4
5 fires increase metal concentrations in surface runoff; however, they did not characterize an event of
6
7 the magnitude of the 2018 Camp Fire.^{17,18,22}
8
9

10
11 One challenge is attributing the presence of metals in runoff to urban sources (burned or
12
13 unburned), directly from wildfire, or to historical land uses. For some elements, such as Al, Fe and
14
15 Mn, it is difficult to ascribe wildland or urban sources, as increases in metals are frequently
16
17 reported after wildland fires due to enrichment in vegetation ash and subsequent mobilization of
18
19 ash and underlying soil during runoff events.^{5,46}
20
21
22

23
24 This study documented significant increases in all metals when comparing the control
25
26 watershed to the burned watersheds, with higher metals concentrations in watersheds that had
27
28 more structures destroyed per urban acre. The increased metal concentrations certainly have
29
30 some dependence on wood ash production. The primary components of wood ash include Ca (13
31
32 – 34%), K (1 – 13%), Mg (0.1 – 9%), Al (0.5 – 1.9%), and Mn (<1%), and Fe (<1%).^{46,47} The metals
33
34 Ca and Mg tend to form carbonate minerals, while Al, Mn, and Fe tend to be in the form of
35
36 oxides.^{46,47} In addition to carbonate minerals and oxides, silicate minerals that include Al, Ca, Fe,
37
38 K, and Mn can be a component of ash, and the presence of phosphate and sulfate minerals (e.g.,
39
40 apatite, gypsum) have also been reported.^{47,48} The observation of increased hardness during early
41
42 season flushing is explained by the presence of the readily dissolved mineral forms while later
43
44 season storms with more energy mobilized the oxide forming, less soluble particulates.⁴⁹
45
46
47
48

49
50 The elevated concentrations of trace metals, their strong correlations with one another and
51
52 with the explanatory variables of the RDA suggest fire-impacted urban areas as likely sources.
53
54 Trace and major elements (i.e., Ba, Cr, Co, Cu, Fe, Mn, Ni, Pb, and Zn) most strongly correlated
55
56
57
58
59
60

1 with each other and with the number of destroyed structures and urban area (%). These RDA
2
3 explanatory variables include urban metal sources, such as automobile components (e.g., frame,
4
5 mechanical and electrical components, material coatings, and tires) and household and
6
7 commercial products (e.g., paints, consumer chemicals, electrical wiring, appliances, and
8
9 electronics).^{48,50,51} Storm runoff samples had concentrations of Co, Cr, Mn, Ni, and Pb that were
10
11 consistently higher than concentrations reported for urban stormwater by a factor of 2–5 (Table 2,
12
13 Figure 4), even though the urban density in Paradise, CA was lower than the >90% developed land
14
15 use in dense urban landscapes.⁵² Wood ash is also known to contain some trace metals with
16
17 toxicity risks that were of interest in this study, such as Cu, Ni, Pb, and Zn. Zn has been reported to
18
19 be as high as 0.2% of some wood ash, but recent studies conducted in a watershed adjacent to
20
21 this study have shown that structure and vehicle ashes have a much greater trace metal content
22
23 than vegetation.^{47,48}
24
25
26
27
28

29
30 Another line of evidence supporting trace elements originating from fire-impacted urban
31
32 areas is the elevated concentrations observed at the urban end-member locations (Little Butte
33
34 Creek Trailer Park and Paul Byrne Aquatic Park), which, unlike routine sampling locations in each
35
36 watershed (Figure 1), did not receive any dilution from non-urban areas in the watershed. The
37
38 samples collected at the end-member locations consistently had the highest metal concentrations
39
40 observed in the study (e.g., Cu >20 $\mu\text{g L}^{-1}$, Pb >5 $\mu\text{g L}^{-1}$, and Zn >1 mg L^{-1} , Table 2). Elevated
41
42 concentrations closer to source materials align with studies reporting that runoff collected from
43
44 automobile fires can be orders of magnitude higher (e.g., 760-1200 $\mu\text{g L}^{-1}$ Cu, 620-2300 $\mu\text{g L}^{-1}$ Pb,
45
46 and 8100 to 11000 $\mu\text{g L}^{-1}$ Zn) than concentrations observed at the end-member locations.¹⁶ It is
47
48 important to note that the dominant materials of construction at the trailer park are different from
49
50 other residential construction (i.e., metal vs. wood construction, lack of foundations).
51
52
53
54
55
56
57
58
59
60

1 Strong consideration was also given to the influence of geological sources including the
2
3 presence of historical, inactive mines as potential sources for trace elements. Dry Creek has the
4
5 largest land area impacted by mine tailings (7%) compared to all other watersheds (<0.5%), and
6
7 the only inactive Mn mines (Table 1). The median Mn concentration in Dry Creek ($192 \mu\text{g L}^{-1}$) was
8
9 almost an order of magnitude higher than in the other burned watersheds (median: $30 \mu\text{g L}^{-1}$),
10
11 which were both higher than in the unburned watershed (median: $9 \mu\text{g L}^{-1}$, Figure 4). Although Dry
12
13 Creek may have a higher likelihood of geologic Mn sources, the urban end-member locations (Little
14
15 Butte Creek Trailer Park and Paul Byrne Aquatic Park) had appreciable median concentrations (75-
16
17 $117 \mu\text{g L}^{-1}$) that support burned, urban sources as well. Additionally, Butte Creek was the only
18
19 watershed with inactive Cr mines (Table 1), but similar Cr concentrations were observed in Clear
20
21 Creek and higher concentrations were observed in Dry Creek and at the two urban end-member
22
23 locations. Correlations between Co, Cr, and Ni could indicate leaching from ultramafic soils.⁵³
24
25 However, ultramafic outcrops are not abundant in the study watersheds, suggesting a
26
27 predominantly anthropogenic source.⁵³ A similar argument can be made for Ba, which could
28
29 originate from the Lovejoy basalt that underlies parts of Butte County.⁵⁴ However, post-fire
30
31 concentrations of Ba in fire-affected watersheds were statistically higher than in the reference
32
33 watershed Big Chico Creek (Figure 4) which also contacts the Lovejoy Basalt, supporting a likely
34
35 anthropogenic origin that mobilized from fire-impacted areas.
36
37
38
39
40
41
42

43 Total Hg was not found to be from the burned urban environment, and instead all Hg
44
45 measurements were attributed to historical gold mining activities. Concentrations upstream of the
46
47 Cherokee mine (1800's era hydraulic mine) were typical for the region, while higher measurements
48
49 in lower Dry Creek (e.g., peak of 665 ng L^{-1}) collected downstream of the mine and the fire can be
50
51 attributed to a residual mine effect and not a fire effect. Total Hg concentrations measured
52
53
54
55
56
57
58
59
60

1 downstream of the fire were within the ranges of concentrations measured in western slope Sierra
2 Nevada streams.⁴⁴ Therefore, although geologic sources cannot be categorically excluded for
3
4 many of the measured metals, trends between watersheds and concentrations at urban end-
5
6 member locations support appreciable anthropogenic sources of metals from the burned urban
7
8 environment, mercury excluded.
9
10
11
12

13 A clear distinction emerged from the RDA showing two groups with different transport
14 behavior based on divergent correlations. The trace metals (Group A) correlated strongly with TSS
15 and with destroyed structures (Figure 9), while having less dependence on the urban area (%).
16
17 These findings potentially indicate the importance of urban burning of houses and vehicles as
18 sources of trace metals in post-fire runoff. The correlation of trace metals with TSS also points to
19
20 particulate-driven transport for most trace metals. Conversely, the major ions and DOC (Group B,
21
22 Figure 8) concentrations had a strong negative correlation with flow and a strong positive
23
24 correlation with urban area (%) (Figure 9). The emergence of Group B points to easily solubilized
25
26 constituents, such as readily dissolved carbonate minerals of Ca and Mg, base anions, and readily
27
28 dissolved organic molecules. The correlations of major ions and DOC with urban area may be
29
30 enhanced due to impervious surfaces increasing the flushing behavior of urban drainages.^{55,56}
31
32 Notably, lower intensity storms immediately after the fire produced lower flows than later storms
33
34 (Figure 3), yet generated higher concentrations of Ca, K, and Mg (Figures S1-S3). This first flush
35
36 behavior for hardness was only observed in Dry and Clear Creeks (Figures S7 and S8), making it
37
38 difficult to clearly separate fire and urban effects. These results suggest that the bulk composition
39
40 of storm runoff highly depends on storm flow energy mobilizing particulates (Group A) and the
41
42 presence of readily dissolved constituents (Group B).⁴⁹
43
44
45
46
47
48
49
50
51
52
53

54 **4.2. Mechanistic Analysis**

55
56
57
58
59
60

1 Most trace metals were present predominantly as particulates (Figure S9), with the only
2 trace metals that did not exhibit a dominant particulate form being Ba, Cu, and Ni. The total
3 concentrations of metals found predominantly in particulate form (i.e., Al, Cr, Co, Fe, Mn, Pb, and
4 Zn) were strongly correlated with the number of destroyed structures and were weakly and
5 inversely correlated with percent urban development (Figure 9). While we did not conduct a
6 mineralogical analysis of the samples, we can briefly speculate on the forms and likely associations
7 of metals based on prior studies and chemical equilibrium modeling. For example, correlations
8 between trace metals and the oxide-forming metals Al, Fe, and Mn, and TSS concentrations
9 suggest that trace metal transport is driven by sorption or co-precipitation on more abundant oxide
10 surfaces. The pH values were circumneutral in all streams, which is known to favor the precipitation
11 of Al (III), Mn (IV), and Fe (III) oxides. Modeling of our results using Visual MINTEQ indeed
12 predicted the formation of Al and Fe oxides, and that conditions would favor Co, Cu, Mg, Ni, Pb,
13 and Zn sorption to oxide surfaces.⁵⁷

14 It is also possible that relationships between oxide-forming metals and trace metals could
15 indicate a shared metal source rather than sorption. Filter-passing Zn concentrations were lower
16 than the method detection limit in 26–74% of samples collected from the mainstem locations but
17 always detected at the urban end-member locations (Table S8). These differences could indicate
18 that the source and transport of Zn after WUI fires are different from typical watershed weathering
19 processes. For instance, Alshehri et al. (2023) found that many metals reported in this study were
20 in nanoparticulate forms within the carbon lattice of ash and co-associated with silicates and
21 carbonate mineral forms.⁴⁸ Further, ash derived from structures and vehicles contained Zn-bearing
22 nanoparticles ranging in size from 50 to 450 nm, which overlaps with the size of Zn nanoparticles
23 used in commercial products such as tire rubbers that contain 1-5% of Zn.⁴⁸ To date, there is no

1 publicly available estimate of the number of destroyed vehicles by the Camp Fire, but if one
2
3
4 assumes one to two vehicles were lost per destroyed structure then the expected number is
5
6 >20,000 (Table 1) and the rubber in burned tires represents a potential source of particulate Zn.
7
8

9 Beyond sorption mechanisms to the mineral phase, it is also possible that metals react with
10
11 the organic carbon fraction of ash. Charred biomass could effectively act as a sorbent due to the
12
13 presence of carboxylic acids, thiols, or amine groups that provide reactive sites within the carbon
14
15 lattice, like activated carbon or biochar.⁵⁸ The particulate organic carbon content of TSS was not
16
17 measured for this study, but this would be an area of interest for future study.
18
19
20

21 Trace metal complexation with DOM is also possible, but no correlations were found
22
23 between DOC and trace metals in this study by Spearman correlation, PCA, or RDA (Figures S10-
24
25 20). The exception was a correlation between Ba and DOC in burned watersheds, though evidence
26
27 of strong Ba-complexation by DOM is limited.^{59,60} The lack of metal-DOC correlation points away
28
29 from this mechanism being a driver of metal transport in this particular system and instead
30
31 suggests metals were particulate-associated.
32
33
34
35

36 **4.3. Consideration of Hydrologic Conditions**

37
38

39 The interpretations of post-fire water quality are acknowledged to be highly dependent on the
40
41 hydrologic conditions within the watersheds studied. While the mean annual precipitation values
42
43 are in good agreement between the pre- and post-fire data in the camp Fire area, timing and
44
45 magnitude of storms also influence the watershed response and downstream water quality.^{61,62}
46
47 The comparison of Butte Creek hydrographs for the two pre- and post-fire water years clearly
48
49 shows that the watershed had similar overall streamflow patterns, including similar peak flows,
50
51 number of storms, and distribution of storms during the year (Figure S25).³⁵ Further, antecedent
52
53
54
55
56
57
58
59
60

1 conditions can greatly influence water quality and watershed responses following periods of wet or
2
3 dry conditions could cause attribution of water composition changes incorrectly attributed to
4
5 wildfire.^{61,62,63} While metal concentrations naturally fluctuate with hydrology, mean annual pre- and
6
7 post-fire water hardness values were statistically indistinguishable in this study. In contrast, post-
8
9 fire trace and major metal concentrations were found to be up to 200-times higher than the
10
11 baseline data. The post-fire data clearly indicates an early season flushing effect of hardness
12
13 metals, but the remaining water-year values are highly consistent with pre-fire concentrations.
14
15 Together, these factors strongly suggest that elevated concentrations of trace metals post-fire were
16
17 outside the range of hydrological variability and can be attributed to fire impacts rather than natural
18
19 concentration fluctuations that would have likely been apparent in hardness metals as well. Further,
20
21 weather in California has high inter-annual and intra-annual variability, and annual fluctuations in
22
23 precipitation timing and quantity can be dramatic. Large fluctuations in antecedent watershed
24
25 conditions make the comparison of water quality data challenging. While acknowledging the
26
27 possibility of hydrologic influence on metal concentrations, the strong agreement in hardness
28
29 concentrations pre- and post-fire, while not a perfect comparison, suggests that the overall water
30
31 quality remained comparable between years, and the large increases in trace metals are likely
32
33 directly due to the fire perturbation.
34
35
36
37
38
39
40

41 **4.4. Other Considerations and Limitations**

42 Samples from drainage areas in close geographic proximity were collected in this study.
43
44 With this side-by-side pairing, there are underlying geologic and vegetation similarities (e.g., conifer
45
46 forests) compared to other wildfire investigations that are geographically diverse. However,
47
48 variability did exist for land use type and burn extent. For example, a greater relative area of Clear
49
50 and Dry Creek watersheds was within the burn area (Figure 1), and these watersheds had higher
51
52
53
54
55
56
57
58
59
60

1 urban development. Therefore, the impacts of both fire and urban development would be expected
2
3 to be amplified in these drainage areas. Although Butte Creek contained the highest number of
4
5 burned structures, it also had the lowest urban area (%) due to its large, upstream portion that has
6
7 low development and was unimpacted by fire. Therefore, the observations in Butte Creek may be
8
9 due to low urban area or the comparatively low fraction of the drainage area that was not burned.
10
11
12

13 Longitudinal sampling within each drainage area could have helped separate some of these
14
15 confounded effects but was not possible in this study. Sampling was limited to locations on the
16
17 lower reaches of each drainage area due to road closures during response and recovery. Another
18
19 impact of access limitations was that one of the end-member sites (i.e., trailer park) could not be
20
21 accessed during the earliest sampling events. The burned materials were exposed to several
22
23 storms before sampling, and concentrations in first flush events may have been higher. First flush
24
25 data are limited in many wildfire studies due to these logistical constraints.⁶⁴ Despite these
26
27 limitations, this study presents a comprehensive dataset with parallel sites, broad water quality
28
29 scope, runoff from burned urban areas, and a time-series capturing different hydrologic flow
30
31 regimes.
32
33
34
35
36

37 **5. Conclusion**

38
39 This study found that the wildland-urban interface impacted by the 2018 Camp Fire
40
41 contributed metals to nearby watersheds at concentrations that could threaten ecosystem health. In
42
43 addition to elevated concentrations of Mn and Fe commonly observed after wildland fires, urban
44
45 burning likely contributed elevated concentrations of Al, Ba, Co, Cr, Cu, Ni, Pb, and Zn from
46
47 anthropogenic fuels such as homes and vehicles.
48
49
50

51
52 The transport of metals was likely controlled by land use features (e.g., impervious surfaces
53
54 in urban environments) and fuel type (e.g., burned structures). Fire-affected creeks draining
55
56
57
58
59
60

1 watersheds with large numbers of burned structures within their urban, impermeable surfaces
2
3 contained the highest concentrations of trace metals.
4
5

6
7 Particulate-associated transport emerged as the primary mechanism responsible for the
8 mobilization of metals, possibly attributed to surface interactions with oxide-forming elements or co-
9 formation with ash during combustion Throughout the sampling campaign, the mobilization and
10 transport of metals were observed, leading to exceedances of EPA criteria. Peak concentrations of
11 Al, Cd, Cu, Ni, Pb, and Zn surpassed both acute and chronic levels of EPA aquatic habitat criteria,
12 persisting from the immediate aftermath six months after the fire. Consequently, the accumulation
13 of metals in riparian sediment may have adversely impacted ecosystems beyond the duration of
14 surface debris removal efforts. These findings underscore the potential for long-term water quality
15 and ecosystem effects resulting from wildfires in the WUI.
16
17
18
19
20
21
22
23
24
25
26
27

28 The study highlights the significant contribution of WUI fires to the long-term effects on water
29 quality and ecosystems, as evidenced by the continued mobilization and accumulation of metals
30 even after the fire has subsided and surface debris has been cleared.
31
32
33
34

35 **Conflicts of Interest**

36
37

38 The authors declare that there are no conflicts of interest.
39
40
41

42 **Acknowledgements**

43

44 We would like to acknowledge and thank the editor and anonymous reviewers for their
45 valuable input and help. Additionally, we gratefully acknowledge our many student-helpers Sean
46 Berriman, Eric Dearden, Robert Gruenberg, John Machado, Yovvani Mojica Perez, Jillian Olivar,
47 Erica Plasencia Campos, Dustin Sears, Brice Vanness, Jamie Villatoro, Andrea Villegas-Fregoso,
48 Gabrielle Wyatt for their field assistance and analytical support. We also thank Radley Ott with
49
50
51
52
53
54
55
56
57
58
59
60

1 Butte County Public Works for assistance with sampling sites access and Cajun James with Sierra
 2 Pacific Industries for lending us autosamplers. This project was funded by an NSF RAPID grant
 3
 4 CBET-1917165. Any use of trade, firm, or product names is for descriptive purposes only and does
 5
 6 not imply endorsement by the U.S. Government.
 7
 8
 9

10 11 **CRedit authorship contribution statement**

12 **Lauren Magliozzi:** investigation, formal analysis, data curation, writing – original draft,
 13 writing – review & editing, visualization; **Sandrine Matiasek:** conceptualization, funding acquisition,
 14 project administration, methodology, validation, investigation, formal analysis, data curation, writing
 15 – original draft, writing – review & editing; **Charles Alpers:** conceptualization, funding acquisition,
 16 resources, methodology, validation, investigation, formal analysis, data curation, writing – original
 17 draft, writing – review & editing; **Julie Korak:** resources, methodology, validation, formal analysis,
 18 writing – original draft, writing – review & editing; **Diane McKnight:** supervision, writing – original
 19 draft, writing – review & editing; **Andrea Foster:** formal analysis, writing – original draft, writing –
 20 review & editing; **Joseph Ryan:** supervision, writing – original draft, writing – review & editing;
 21 **Peijia Ku:** investigation, formal analysis, writing – original draft, writing – review & editing; **Martin**
 22 **Tsz-Ki Tsui:** resources, investigation, formal analysis, writing – original draft, writing – review &
 23 editing; **Alex Chow:** writing – original draft, writing – review & editing; **Jackson Webster:**
 24 conceptualization, funding acquisition, project administration, methodology, validation,
 25 investigation, formal analysis, data curation, writing – original draft, writing – review & editing
 26
 27
 28
 29

30 **References**

- 31 1. NatCatSERVICE, Munich Re, Natural Catastrophes in 2018,
 32 [https://www.munichre.com/content/dam/munichre/contentlounge/website-](https://www.munichre.com/content/dam/munichre/contentlounge/website-pieces/documents/munichre-natural-catastrophes-in-2018.pdf)
 33 [pieces/documents/munichre-natural-catastrophes-in-2018.pdf](https://www.munichre.com/content/dam/munichre/contentlounge/website-pieces/documents/munichre-natural-catastrophes-in-2018.pdf) (accessed 2022).
- 34 2. A. Maranghides, E. D. Link, C. U. Brown, W. Mell, S. Hawks, M. Wilson, W. Brewer, C. Brown, B.
 35 Vihnaneck and W. D. Walton, A case study of the Camp Fire - Fire progression timeline, Technical
 36 Note, *National Institute of Standards and Technology*, Gaithersburg, MD, 2021.
 37 <https://doi.org/10.6028/NIST.TN.2135>
- 38 3. C. C. Rhoades, J. P. Nunes, U. Silins and S. H. Doerr, The influence of wildfire on water quality and
 39 watershed processes: new insights and remaining challenges, *Int. J. Wildland Fire*, 2019, **28**, 721–
 40 725. https://doi.org/10.1071/WFv28n10_FO
- 41 4. L. F. DeBano, *Water repellent soils: a state-of-the-art*, USDA Forest Service General Technical
 42 Report PSW-46, Pacific Southwest Forest and Range Experimental Station, Berkeley, California,
 43 USA, 1981.
- 44 5. H. G. Smith, G. J. Sheridan, P. N. J. Lane, P. Nyman and S. Haydon, Wildfire effects on water
 45 quality in forest catchments: A review with implications for water supply, *J. Hydrol.*, 2011, **396**, 170–
 46 192. <https://doi.org/10.1016/j.jhydrol.2010.10.043>
- 47 6. M. Parise and S. H. Cannon, Wildfire impacts on the processes that generate debris flows in burned
 48 watersheds, *Nat. Hazards*, 2012, **61**, 217–227. <https://doi.org/10.1007/s11069-011-9769-9>
- 49 7. A. J. Rust, T. S. Hogue, S. A. Saxe and J. A. McCray, Post-fire water-quality response in the western
 50 United States, *Int. J. Wildland Fire*, 2018, **27**, 203–216. <https://doi.org/10.1071/WF17115>
- 51
52
53
54
55
56
57
58
59
60

- 1 8. J. Abraham, K. Dowling and S. Florentine, Risk of post-fire metal mobilization into surface water
2 resources: A review, *Sci. Total Environ.*, 2017, **599**, 1740–1755.
3 <https://doi.org/10.1016/j.scitotenv.2017.05.096>
4
- 5 9. T. B. Hampton, S. Lin and N. B. Basu, Forest fire effects on stream water quality at continental
6 scales: a meta-analysis, *Environ. Res. Lett.*, 2022, **17**, 064003. <https://doi.org/10.1088/1748-9326/ac6a6c>
7
- 8 10. K. O. Odigie and A. R. Flegal, Pyrogenic remobilization of historic industrial lead depositions,
9 *Environ. Sci. Technol.*, 2011, **45**, 6290–6295. <https://doi.org/10.1021/es200944w>
10
- 11 11. R. E. Wolf, S. A. Morman, P. L. Hageman, T. M. Hoefen and G. S. Plumlee, Simultaneous speciation
12 of arsenic, selenium, and chromium: Species stability, sample preservation, and analysis of ash and
13 soil leachates, *Anal. Bioanal. Chem.*, 2011, **401**, 2733–2745. <https://doi.org/10.1007/s00216-011-5275-x>
14
15
- 16 12. Y. Ma, P. Egodawatta, J. McGree, A. Liu and A. Goonetilleke, Human health risk assessment of
17 heavy metals in urban stormwater, *Sci. Total Environ.*, 2016, **557**, 764–772.
18 <https://doi.org/10.1016/j.scitotenv.2016.03.067>
19
- 20 13. N. R. Jyothi, Heavy metal sources and their effects on human health, in *Heavy Metals: Their
21 Environmental Impacts and Mitigation*, eds. M. Nazal and H. Zhao, IntechOpen, London, UK, 2021,
22 21–32. <https://doi.org/10.5772/intechopen.91574>
- 23 14. V. C. Radeloff, D. P. Helmers, H. A. Kramer, M. H. Mockrin, P. M. Alexandre, A. Bar-Massada, V.
24 Butsic, T. J. Hawbaker, S. Martinuzzi, A. D. Syphard and S. I. Stewart, Rapid growth of the US
25 wildland-urban interface raises wildfire risk, *Proc. Natl. Acad. Sci. U.S.A.*, 2018, **115**, 3314–3319.
26 <https://doi.org/10.1073/pnas.1718850115>
27
- 28 15. G. S. Plumlee, S. A. Morman, G. P. Meeker, T. M. Hoefen, P. L. Hageman and R. E. Wolf, The
29 environmental and medical geochemistry of potentially hazardous materials produced by disasters,
30 in *Treatise on Geochemistry*, eds. H. D. Holland and K. K. Turekian, Elsevier, second edn., 2014, 11-
31 7, 257-304. <https://doi.org/10.1016/B978-0-08-095975-7.00907-4>
32
- 33 16. A. Lönnemark and P. Blomqvist, Emissions from an automobile fire, *Chemosphere*, 2006, **62**, 1043–
34 1056. <https://doi.org/10.1016/j.chemosphere.2005.05.002>
- 35 17. E. D. Stein, J. S. Brown, T. S. Hogue, M. P. Burke and A. Kinoshita, Stormwater contaminant loading
36 following southern California wildfires, *Environ. Toxicol. Chem.*, 2012, **31**, 2625–2638.
37 <https://doi.org/10.1002/etc.1994>
38
- 39 18. M. P. Burke, T. S. Hogue, A. M. Kinoshita, J. Barco, C. Wessel and E. D. Stein, Pre- and post-fire
40 pollutant loads in an urban fringe watershed in Southern California, *Environ. Monit. Assess.*, 2013,
41 **185**, 10131–10145. <https://doi.org/10.1007/s10661-013-3318-9>
42
- 43 19. G. S. Plumlee, D. A. Martin, T. Hoefen, R. Kokaly, P. Hageman, A. Eckberg, G. P. Meeker, M.
44 Adams, M. Anthony and P. J. Lamothe, Preliminary analytical results for ash and burned soils from
45 the October 2007 southern California Wildfires, *U.S. Geological Survey Open-File Report*, 2007,
46 **1407**, 15 p. <https://doi.org/10.3133/ofr20071407>
47
- 48 20. A. A. Stec, K. Dickens, J. L. J. Barnes and C. Bedford, Environmental contamination following the
49 Grenfell Tower fire, *Chemosphere*, 2019, **226**, 576–586.
50 <https://doi.org/10.1016/j.chemosphere.2019.03.153>
- 51 21. G. O. Mendez, Water-quality data from storm runoff after the 2007 fires, San Diego County,
52 California, *U.S. Geological Survey Open-File Report*, 2010, **1234**, 8 p.
53 <https://pubs.er.usgs.gov/publication/ofr20101234>
54
55
56
57
58
59
60

22. C. A. Burton, T. M. Hoefen, G. S. Plumlee, K. L. Baumberger, A. R. Backlin, E. Gallegos and R. N. Fisher, Trace elements in stormflow, ash, and burned soil following the 2009 Station Fire in southern California, *PloS One*, 2016, **11**, 1–26 <https://doi.org/10.1371/journal.pone.0153372>
23. J. R. Lead and K. J. Wilkinson, Aquatic colloids and nanoparticles: current knowledge and future trends, *Environ. Chem.*, 2006, **3**, 159–171. <https://doi.org/10.1071/EN06025>
24. G. R. Aiken, H. Hsu-Kim, J. N. Ryan, Influence of dissolved organic matter on the environmental fate of metals, nanoparticles, and colloids, *Environ. Sci. Technol.*, 2011, **45**, 3196-3201. <https://doi.org/10.1021/es103992s>
25. L. Hare, Aquatic insects and trace metals: bioavailability, bioaccumulation, and toxicity, *Crit. Rev. Toxicol.*, 1992, **22**, 327–369. <https://doi.org/10.3109/10408449209146312>
26. H. Blanck, W. Admiraal, R. F. M. J. Cleven, H. Guasch, M. A. G. T. van den Hoop, N. Ivorra, B. Nyström, M. Paulsson, R. P. Petterson, S. Sabater and G. M. J. Tubbing, Variability in zinc tolerance, measured as incorporation of radio-labeled carbon dioxide and thymidine, in periphyton communities sampled from 15 European river stretches, *Arch. Environ. Contam. Toxicol.*, 2003, **44**, 17–29. <https://doi.org/10.1007/s00244-002-1258-4>
27. M. C. Watzin and P. R. Roscigno, The effects of zinc contamination on the recruitment and early survival of benthic invertebrates in an estuary, *Mar. Pollut. Bull.*, 1997, **34**, 443–455. [https://doi.org/10.1016/S0025-326X\(96\)00132-4](https://doi.org/10.1016/S0025-326X(96)00132-4)
28. P. R. Paquin, J. W. Gorsuch, S. Apte, G. E. Batley, K. C. Bowles, P. G. C. Campbell, C. G. Delos, D. M. Di Toro, R. L. Dwyer, F. Galvez, R. W. Gensemer, G. G. Goss, C. Hogstrand, C. R. Janssen, J. C. McGeer, R. B. Naddy, R. C. Playle, R. C. Santore, U. Schneider, W. A. Stubblefield, C. M. Wood and K. B. Wu, The biotic ligand model: A historical overview, *Comp. Biochem. Physiol., Part C: Toxicol. Pharmacol.*, 2002, **133**, 3–35. [https://doi.org/10.1016/S1532-0456\(02\)00112-6](https://doi.org/10.1016/S1532-0456(02)00112-6)
29. D. W. Burkett and A. E. Conlin, *Soil Survey of Butte Area, California, Parts of Butte and Plumas Counties*. United States Department of Agriculture, Natural Resources Conservation Service, 2006.
30. California Department of Conservation, Division of Land Resource Protection, Farmland Mapping and Monitoring Program, *Butte County Important Farmland*, Downloadable Data, 1988-2020. https://maps.conservation.ca.gov/dlrp/metadata/importantfarmland/butte_meta.htm, (accessed November 2022).
31. California Department of Forestry and Fire Protection, Camp Fire Structure Status Map, 2020, <https://frap.fire.ca.gov/mapping/gis-data>, (accessed November 2022).
32. California Geological Survey, Geologic Map of California, 2010, <https://www.arcgis.com/home/item.html?id=2a718c86c96e41e298410c8b58515812>, (accessed November 2022).
33. California Department of Conservation, Mines Online (MOL), <https://maps.conservation.ca.gov/mol/index.html>, (accessed November 2022).
34. U.S. Geological Survey, 2016, National Water Information System, USGS Water Data for the Nation, <https://waterdata.usgs.gov/monitoring-location/11390000/>, (accessed November 2023).
35. U.S. Geological Survey, 2019, The StreamStats program, <https://streamstats.usgs.gov/ss/>, (accessed July 2023).
36. California Department of Water Resources, California Data Exchange Center, <https://cdec.water.ca.gov>, (accessed November 2022).
37. P. A. Lydon, Geology and lahars of the Tuscan Formation, northern California, *Mem. - Geol. Soc. Am.*, 1968, **116**, 441–476. <https://doi.org/10.1130/MEM116-p441>

- 1 38. U.S. Geological Survey, Mineral Resources Data System (MRDS), <https://mrdata.usgs.gov/mrds/>,
2 (accessed November 2022).
- 3
- 4 39. D. L. Brown, Cherokee watershed water quality report, 2005, Prepared for Butte County, CA. 84 pp.
- 5
- 6 40. C. N. Alpers, D. A. Roth, K. D. Scheiderich, J. P. Webster and S. J. Matiasek. Geochemical data for
7 post-fire surface water from areas affected by the 2018 Camp Fire, Butte County, California, USGS
8 Data Release (IP-134247). <https://doi.org/10.5066/P9XOMVMH>
- 9
- 10 41. R Core Team, R: A language and environment for statistical computing (v4.2.1), R Foundation for
11 Statistical Computing, Vienna, Austria, 2022. <https://www.R-project.org/>
- 12 42. B. Schloerke, D. Cook, J. Larmarange, F. Briatte, M. Marbach, E. Thoen, A. Elberg and J. Crowley,
13 GGally R package v2.1.2, <https://cran.r-project.org/web/packages/GGally/index.html> (accessed
14 2021).
- 15 43. J. Oksanen, G. L. Simpson, F. G. Blanchet, R. Kindt, P. Legendre, P. R. Minchin, R. B. O'Hara, P.
16 Solymos, M. H. H. Stevens, E. Szoecs, H. Wagner, M. Barbour, M. Bedward, B. Bolker, D. Borcard,
17 G. Carvalho, M. Chirico, M. De Caceres, S. Durand, H. B. A. Evangelista, R. FitzJohn, M. Friendly,
18 B. Furneaux, G. Hannigan, M. O. Hill, L. Lahti, D. McGlenn, M.-H. Ouellette, E. Ribeiro Cunha, T.
19 Smith, A. Stier, C. J. F. Ter Braak and J. Weedon, vegan R package v2.6-2, [https://cran.r-](https://cran.r-project.org/web/packages/vegan/index.html)
20 [project.org/web/packages/vegan/index.html](https://cran.r-project.org/web/packages/vegan/index.html) (accessed October 2022).
- 21
- 22 44. J. A. Davis, W. A. Heim, A. Bonnema, B. Jakl and D. Yee, Mercury and methylmercury in fish and
23 water from the Sacramento-San Joaquin Delta: August 2016 - April 2017, *Delta Regional Monitoring*
24 *Program Report*, 2018, 54 p.
25 <https://www.noaa.gov/sites/default/files/legacy/document/2020/Oct/07354626186.pdf>.
- 26
- 27 45. U.S. Environmental Protection Agency, National Recommended Water Quality Criteria,
28 <https://www.epa.gov/wqc/national-recommended-water-quality-criteria-aquatic-life-criteria-table>,
29 (accessed November 2022).
- 30
- 31 46. M. B. Bodí, D. A. Martín, V. N. Balfour, C. Santín, S. H. Doerr, P. Pereira, A. Cerdà and J. Mataix-
32 Solera, Wildland fire ash: Production, composition and eco-hydro-geomorphic effects, *Earth-Sci.*
33 *Rev.*, 2014, **130**, 103–127. <https://doi.org/10.1016/j.earscirev.2013.12.007>
- 34 47. A. Rahman, E. El Hayek, J. M. Blake, R. J. Bixby, A. M. Ali, M. Spilde, A. A. Otieno, K. Miltenberger,
35 C. Ridgeway, K. Artyushkova and V. Atudorei, Metal reactivity in laboratory burned wood from a
36 watershed affected by wildfires, *Environ. Sci. Technol.* 2018, **52**, 8115-23.
37 <https://doi.org/10.1021/acs.est.8b00530>
- 38
- 39 48. T. Alshehri, J. Wang, S. A. Singerling, J. Gigault, J. P. Webster, S. J. Matiasek, C. N. Alpers and M.
40 Baalousha, Wildland-urban interface fire ashes as a major source of incidental nanomaterials, *J.*
41 *Hazard. Mater.* 2023, **443**, 130311. <https://doi.org/10.1016/j.jhazmat.2022.130311>
- 42
- 43 49. R. M. Harrison and S. J. Wilson, The chemical composition of highway drainage waters I. Major ions
44 and selected trace metals, *Sci. Total Environ.*, 1985, **43**, 63-77.
- 45 50. H. W. Mielke, C. R. Gonzales, E. Powell, A. Shah and P. W. Mielke, Natural and anthropogenic
46 processes that concentrate Mn in rural and urban environments of the Lower Mississippi River Delta,
47 *Environ. Res.*, 2002, **90**, 157–168. <https://doi.org/10.1006/enrs.2002.4382>
- 48
- 49 51. J. K. Gietl, R. Lawrence, A. J. Thorpe and R. M. Harrison, Identification of brake wear particles and
50 derivation of a quantitative tracer for brake dust at a major road, *Atmos. Environ.*, 2010, **44**, 141–
51 146. <https://doi.org/10.1016/j.atmosenv.2009.10.016>
- 52
- 53 52. J. R. Masoner, D. W. Kolpin, I. M. Cozzarelli, L. B. Barber, D. S. Burden, W. T. Foreman, K. J.
54 Forshay, E. T. Furlong, J. F. Groves, M. L. Hladik, M. E. Hopton, J. B. Jaeschke, S. H. Keefe, D. P.
55 Krabbenhoft, R. Lowrance, K. M. Romanok, D. L. Rus, W. R. Selbig, B. H. Williams and P. M.
- 56
- 57
- 58
- 59
- 60

- 1
2
3
4
5
6
7
8
9
10
11
12
13
14
15
16
17
18
19
20
21
22
23
24
25
26
27
28
29
30
31
32
33
34
35
36
37
38
39
40
41
42
43
44
45
46
47
48
49
50
51
52
53
54
55
56
57
58
59
60
- Bradley, Urban stormwater: An overlooked pathway of extensive mixed contaminants to surface and groundwaters in the United States, *Environ. Sci. Technol.*, 2019, **53**, 10070–10081. <https://doi.org/10.1021/acs.est.9b02867>
53. A. M. Stueber and G. G. Goles, Abundances of Na, Mn, Cr, Sc and Co in ultramafic rocks, *Geochim. Cosmochim. Acta*, 1967, **31**, 75–93. [https://doi.org/10.1016/0016-7037\(67\)90099-3](https://doi.org/10.1016/0016-7037(67)90099-3)
54. Q. L. Street, Regional paleo-topographic setting of the Lovejoy Basalt, northern California, MSc thesis, California State University Chico, 2009. <https://scholarworks.calstate.edu/concern/theses/6d56zx17z>
55. G. W. Characklis and M. R. Wiesner, Particles, metals, and water quality in runoff from large urban watershed, *J. Environ. Eng.*, 1997, **123**, 753-9.
56. J. J. Sansalone and S. G. Buchberger, Partitioning and first flush of metals in urban roadway storm water, *J. Environ. Eng.*, 1997, **123**, 134-43.
57. J. P. Gustafsson, Visual MINTEQ ver. 3.1 [Computer software], 2013, KTH Royal Institute of Technology, <https://vminteq.lwr.kth.se/>
58. H. Li, X. Dong, E. B. da Silva, L. M. de Oliveira, Y. Chen and L.Q. Ma, Mechanisms of metal sorption by biochars: Biochar characteristics and modifications. *Chemosphere*, 2017, **178**, 466-78. <https://doi.org/10.1016/j.chemosphere.2017.03.072>
59. V. Cappuyns, Barium (Ba) leaching from soils and certified reference materials, *J. Appl. Geochem.* 2018, **88**, 68-84. <https://doi.org/10.1016/j.apgeochem.2017.05.002>
60. Y. Yi, M. Xiao, K. M. G. Mostofa, S. Xu and Z. Wang, Spatial variations of trace metals and their complexation behavior with DOM in the water of Dianchi Lake, China, *Int. J. Environ. Res. Public Health*, 2019, **16**, 4919. <https://doi.org/10.3390/ijerph16244919>
61. F. Z. Maina and E. R. Siirila-Woodburn, Watersheds dynamics following wildfires: Nonlinear feedbacks and implications on hydrologic responses, *Hydrol. Process.*, 2020, **34**, 33-50, <https://doi.org/10.1002/hyp.13568>
62. F. Z. Maina, E. R. Siirila-Woodburn, M. Newcomer, Z. Xu and C. Steefel, Determining the impact of a severe dry to wet transition on watershed hydrodynamics in California, USA with an integrated hydrologic model, *J. Appl. Hydrol.*, 2020, **580**, 124358. <https://doi.org/10.1016/j.jhydrol.2019.124358>
63. M. E. Newcomer, J. Underwood, S. F. Murphy, C. Ulrich, T. Schram, S. R. Maples, J. Peña, E. R. Siirila-Woodburn, M. Trotta, J. Jasperse and D. Seymour, Prolonged drought in a northern California coastal region suppresses wildfire impacts on hydrology, *Water Resour. Res.*, 2023, **58** 034206. <https://doi.org/10.1029/2022WR034206>
64. O. D. Raelison, R. Valenca, A. Lee, S. Karim, J. P. Webster, B. A. Poulin and S. K. Mohanty, Wildfire impacts on surface water quality parameters: Cause of data variability and reporting needs, *Environ. Pollut.*, 2023, **317**, 120713. <https://doi.org/10.1016/j.envpol.2022.120713>

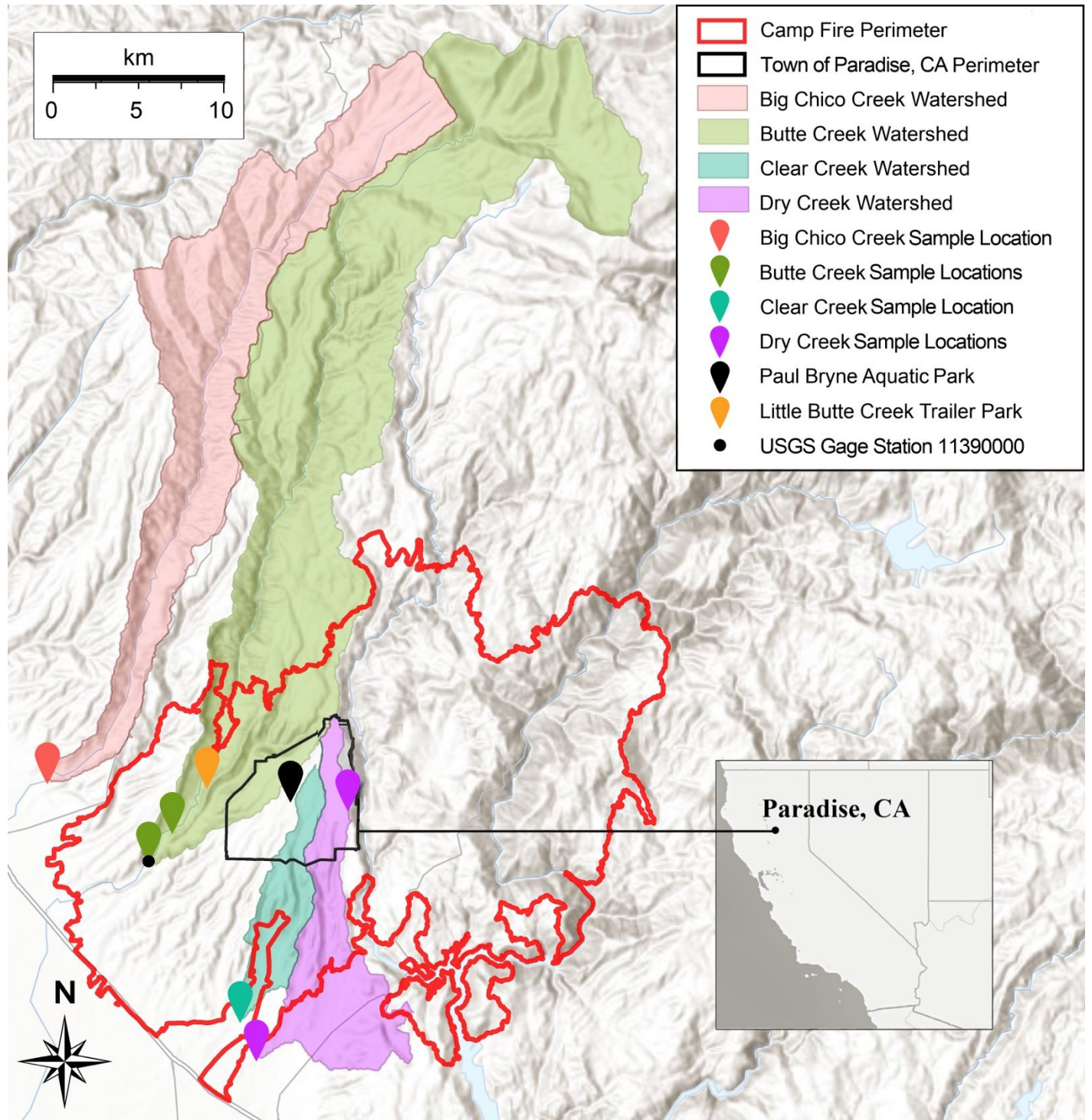


Figure 1. Map of watersheds, sampling locations (markers) in each watershed, Town of Paradise limits (black line), and the 2018 Camp Fire perimeter (red line). The inset map displays the Town of Paradise within California. The Butte Creek stream gage is located next to the western-most sampling point in the Butte Creek watershed.



Figure 2. Photographs of the effects of the Camp Fire taken January 2019: a.) Burned vehicle from Ginny Lane in the Town of Paradise, CA. b.) Little Butte Creek Trailer Park post-fire, looking east. c.) Stormwater moving through ashes of burned Little Butte Creek Trailer Park. Same time and location as photo c, looking west.

Table 1. Characteristics of the study watersheds include watershed area in hectares, percentage of area burned in the Camp Fire, number of burned structures, percentage of urban and forested areas, percentage of mined land-use area, and number of closed Au, Cr, or Mn mines.

Watershed	Area (Hectares)	Burn Area (%)	Burned Structures (#)	Urban Area (%)	Forest Area (%)	Mined Area (%)	Closed Mines (#)		
							Au	Cr	Mn
Big Chico Creek	200,048	0.0	0	1.2	69	0.0	2	0	0
Butte Creek	40,406	16	6,634	3.7	69	0.3	81	9	0
Clear Creek	3,170	78	2,454	18	31	0.0	0	0	0
Dry Creek	6,737	46	3,820	9.0	33	7.0	16	0	2

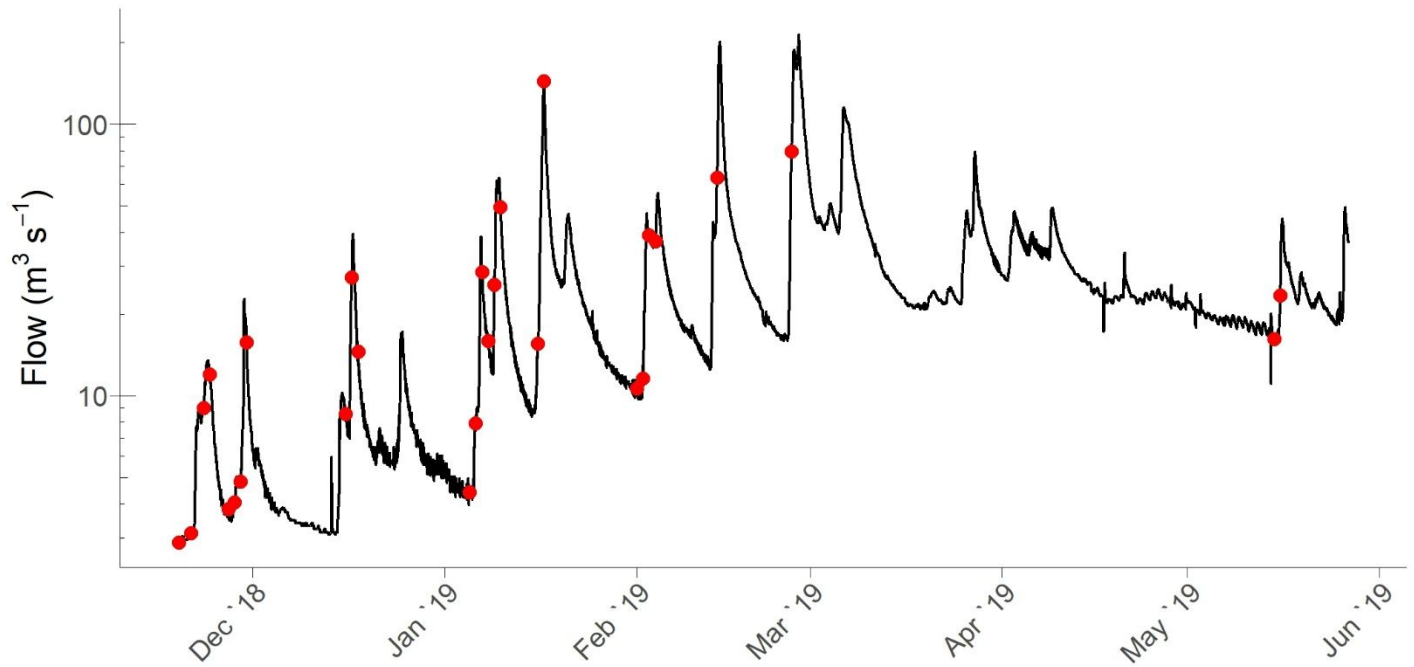


Figure 3. Butte Creek hydrograph from Butte Creek gaging station (USGS #11390000) from November 2018 to June 2019. Red dots indicate sampling events.

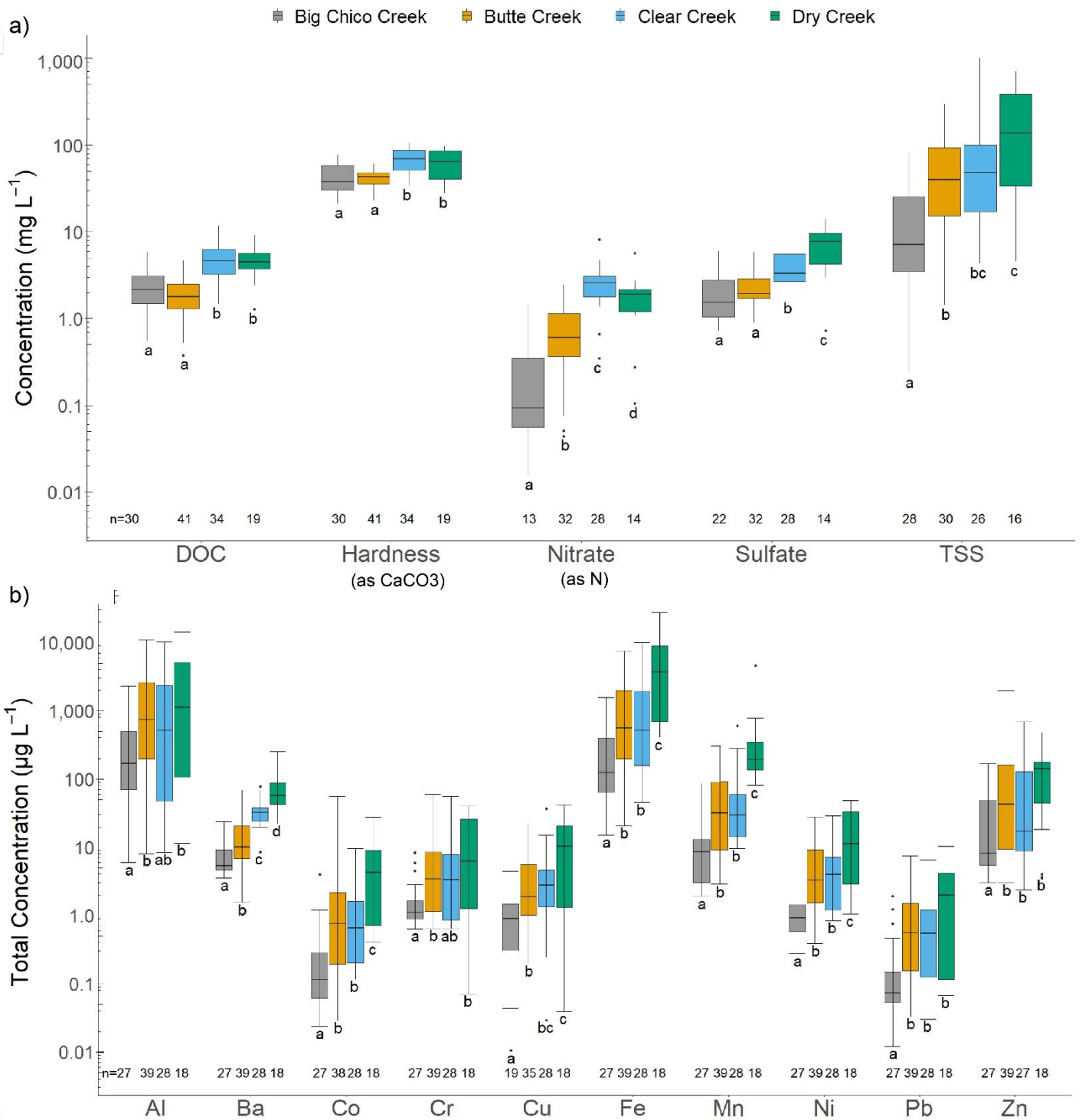


Figure 4. a) Box plots of DOC, hardness (as CaCO_3), nitrate (as N), sulfate, and TSS in each watershed (mg/L). b) Box plots of total metal concentrations measured in each watershed ($\mu\text{g/L}$). Watersheds are displayed in order of increasing number of destroyed structures per urban area. Boxes show 25% and 75% quartiles with the center line at the median of the dataset. The whiskers extend to 5% and 95%, and outliers extend outside of the whiskers. Letters beneath bars show results of Wilcoxon U test. Number of samples for each watershed are listed on the bottom of the y-axis.

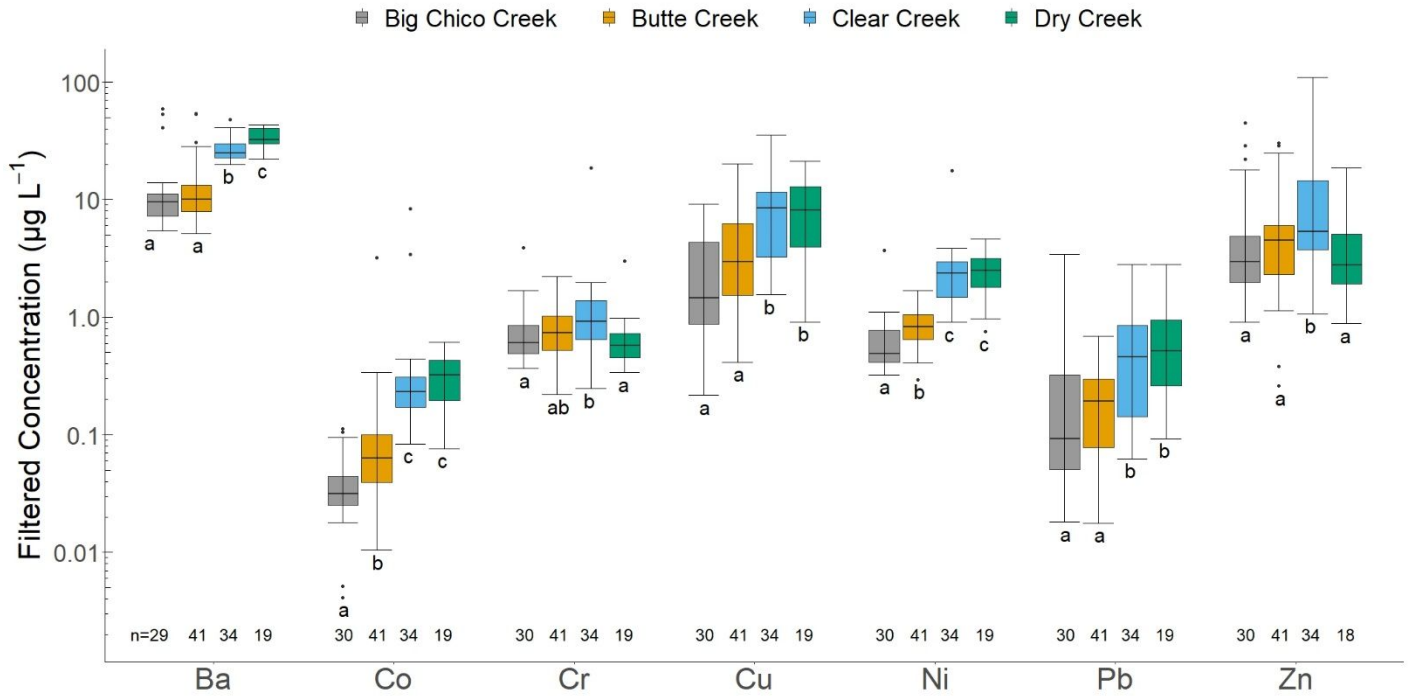


Figure 5. Box plots of filtered metal concentrations measured in each watershed (µg/L). Only metals that have detections for at least 20% of filtered samples are included. Boxes show 25% and 75% quartiles with the center line at the median of the dataset. The whiskers extend to 5% and 95%, and outliers extend outside of the whiskers. Letters beneath bars show results of Wilcoxon U test. Number of samples for each watershed are listed on the bottom of the y-axis.

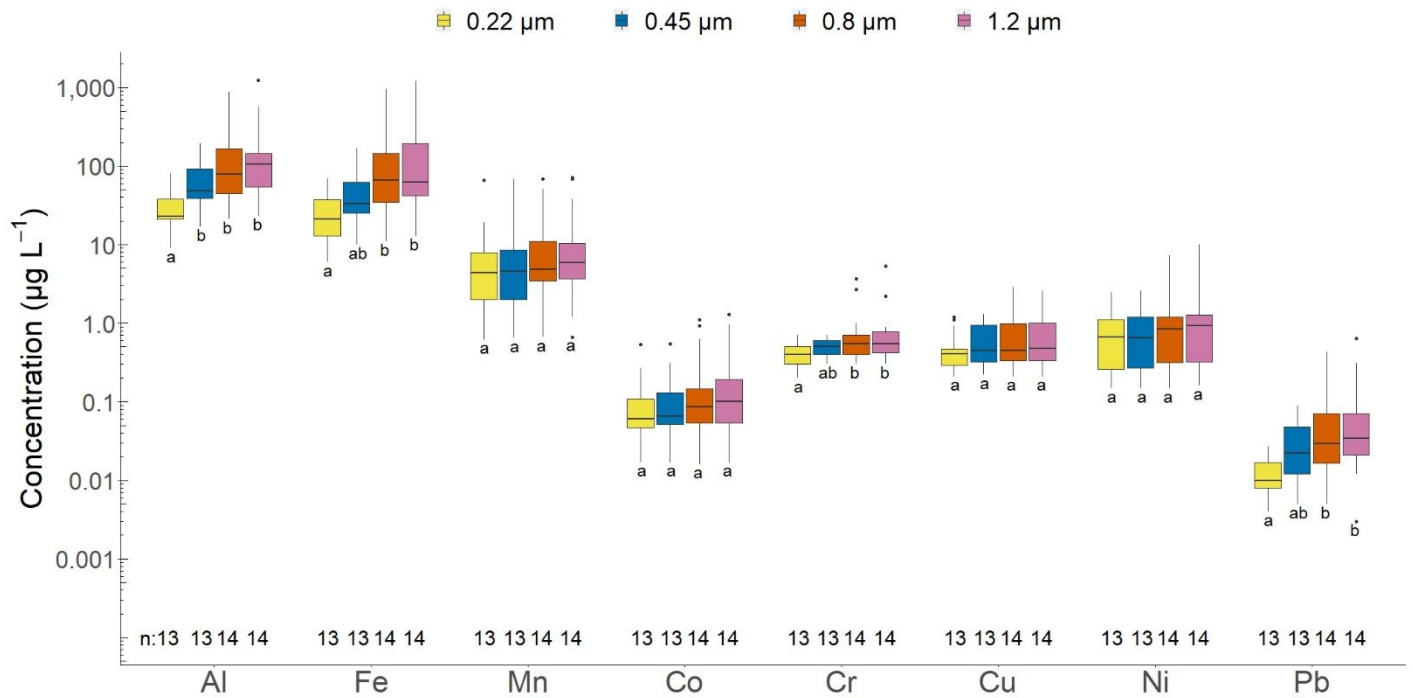


Figure 6. Box plots of metal concentrations from all watersheds after filtration using pore sizes of 0.22, 0.45, 0.8, and 1.2 μm ⁴⁰. Boxes show 25% and 75% quartiles with the center line at the median of the dataset. The whiskers extend to 5% and 95%, and outliers extend outside of the whiskers. Letters beneath bars show results of Wilcoxon U test. Number of samples for each filter size are listed on the bottom of the y-axis.

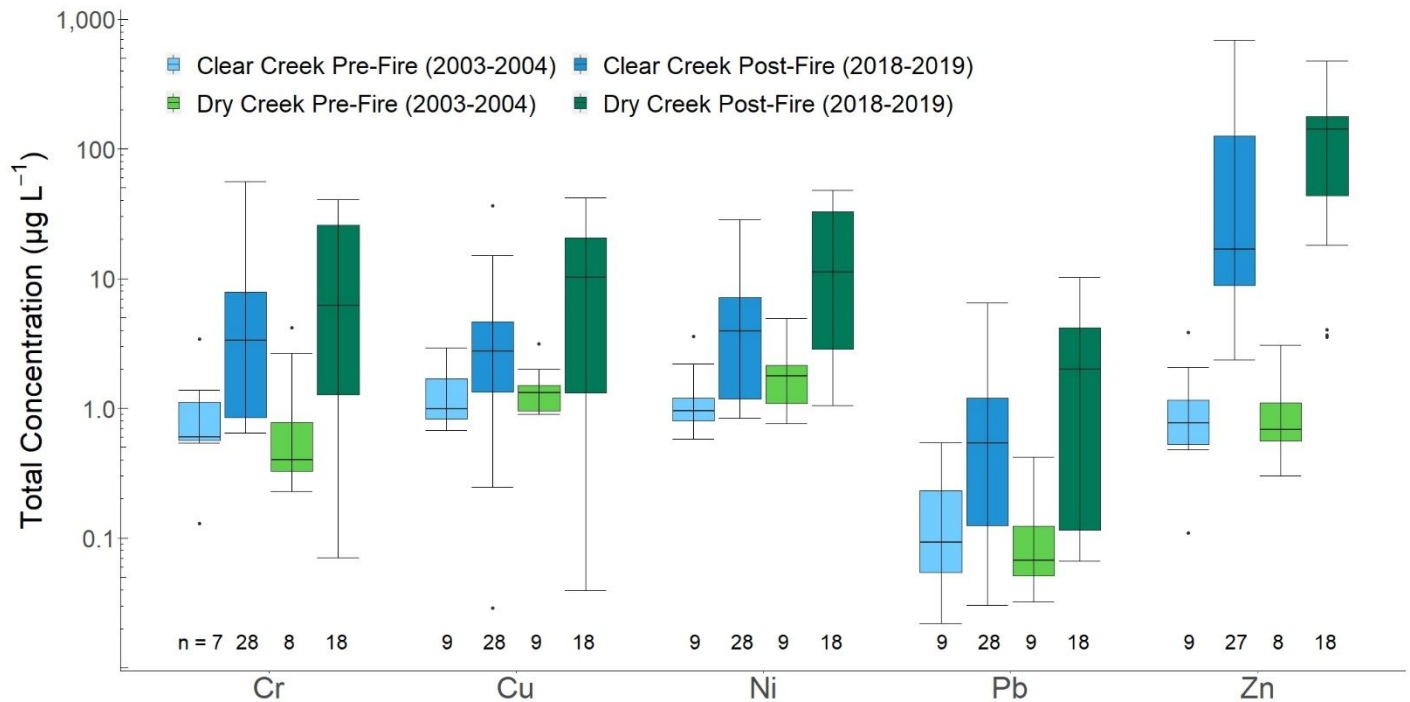


Figure 7. Total concentration (µg/L) of metals in Clear Creek and Dry Creek before and after the Camp Fire (2018-2019).³⁹ Boxes show 25% and 75% quartiles with the center line at the median of the dataset. The whiskers extend to 5% and 95%, and outliers extend outside of the whiskers. Number of samples for each watershed are listed on the bottom of the y-axis.

Table 2. Summary of the number of exceedances of EPA aquatic life criteria peak recommendations (acute and chronic) for each metal and watershed. Total and Filter-Passing (F-P) fractions are presented. Pb and Ni results are located in Table S13. The no. fold increase is the maximum concentration divided by the limit. A dash (-) is presented when there were no exceedances.

Metal	Sample Location	Sample Type	Aquatic Habitat Recommendation: Acute				Aquatic Habitat Recommendation: Chronic			
			No. of Exceeds.	No. Fold Increase	Max. Conc. (ppb)	Limit (ppb)	No. of Exceeds.	No. Fold Increase	Max. Conc. (ppb)	Limit (ppb)
Al	Aquatic Park	Total	2	6.7	5000	750	4	58	5004	87
	Big Chico Creek	F-P	-	-	-	-	2	1.7	145	87
		Total	4	3.1	2300	750	19	26	2304	87
	Butte Creek	F-P	-	-	-	-	9	1.8	153	87
		Total	22	21	15900	750	36	180	15893	87
	Clear Creek	F-P	-	-	-	-	16	6.1	528	87
		Total	13	14	10300	750	19	120	10254	87
	Dry Creek	Total	9	19	14200	750	14	16	14195	87
Little Butte Creek Trailer Park	F-P	-	-	-	-	1	3.9	338	87	
	Total	1	3.6	2670	750	1	3.1	2668	87	
Cd	Butte Creek	Total	1	3.50	2.86	0.8	1	5.8	2.86	0.49
Cu	Aquatic Park	F-P	3	3.9	8.13	2.1	3	3.3	8.94	2.74
		Total	3	8.4	24.4	2.9	3	8.6	24.4	2.85
	Big Chico Creek	F-P	5	1.8	7.49	4.1	8	2.0	7.49	3.20
		Total	10	3.8	13.2	3.5	13	3.2	22.6	7.30
	Butte Creek	F-P	17	4.2	20.2	4.9	24	5.5	20.2	3.65
		Total	4	3.7	36.6	8.2	5	5.3	36.6	6.88
	Clear Creek	F-P	14	7.3	35.5	4.9	20	9.7	35.5	3.65
		Total	8	4.0	21.3	5.3	10	5.8	21.3	3.65
	Dry Creek	F-P	9	7.1	33.3	4.7	10	65	33.3	5.16
		Total	1	2.0	25.0	13	1	2.5	25.0	10.1
Little Butte Creek Trailer Park	F-P	2	11	8.30	7.3	2	16	13.4	8.18	
	Total	1	2.2	81.0	36	1	2.2	81.0	36.5	
Zn	Aquatic Park	F-P	1	2.2	81.0	36	1	2.2	81.0	36.5
		Total	3	7.0	258	22	3	11	258	22.5
	Big Chico Creek	Total	6	3.4	166	41	5	4.0	166	41.6
	Butte Creek	Total	19	52	1943	69	18	15	1017	69.7
	Clear Creek	F-P	2	1.3	87.0	70	2	1.2	87.0	71.3
		Total	9	14	693	51	9	13	693	51.8
	Dry Creek	Total	11	11	478	44	11	11	451	45.0
	Little Butte Creek Trailer Park	Total	1	1.0	1079	110	1	9.8	1079	110

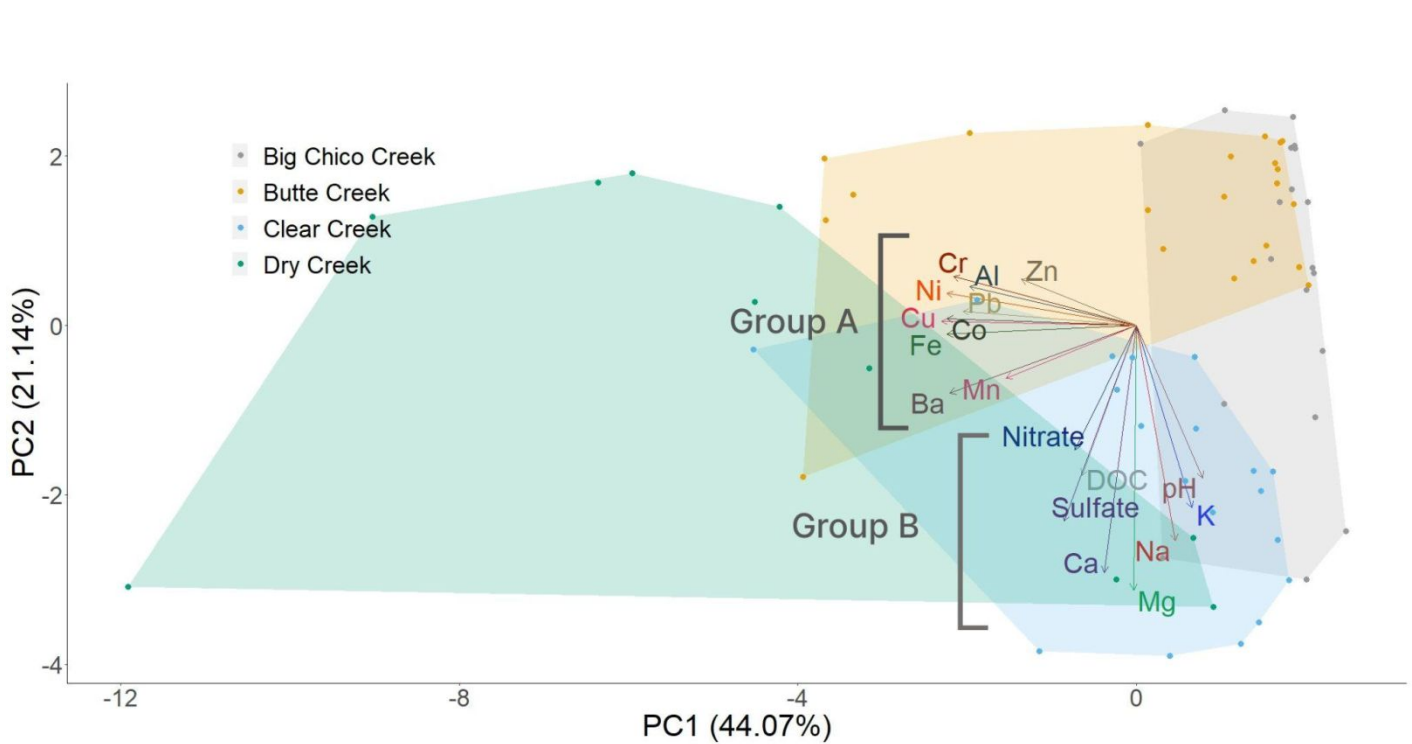


Figure 8. Principal component analysis (PCA) of all watersheds (Big Chico Creek, Butte Creek, Clear Creek, and Dry Creek) including total trace metal concentrations, major cations, DOC, sulfate, nitrate, and pH. Each point represents a discrete sampling event and shaded areas confine discrete samples within each watershed. Group designations outline two central tendencies of the data, where Group A includes trace metals (Al, Ba, Cu, Co, Cr, Fe, Mn, Ni, Pb, and Zn) and Group B includes major ions Ca, K, Mg, Na, nitrate, and sulfate, pH, and DOC.

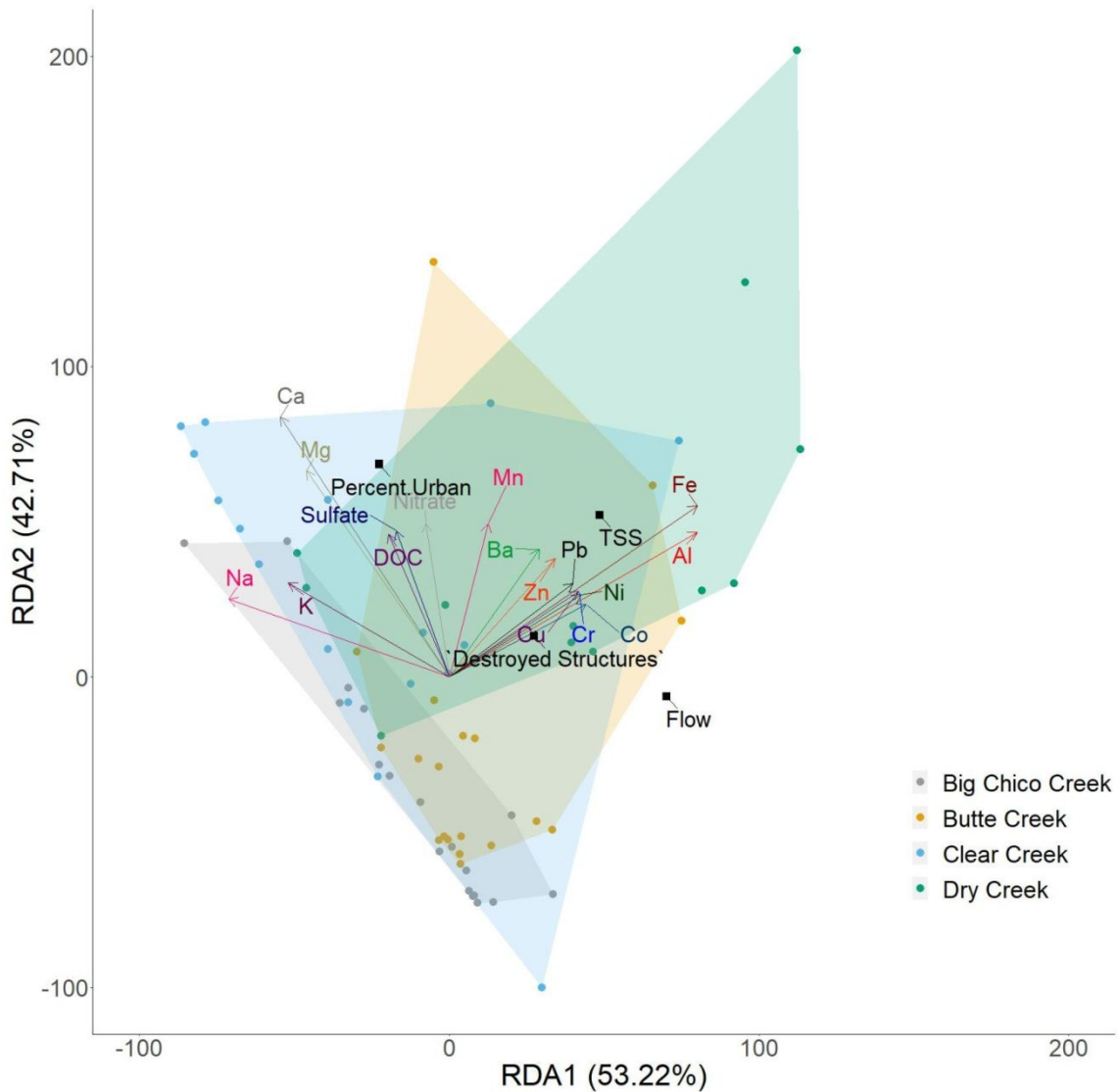


Figure 9. Redundancy analysis (RDA) of all watersheds (Big Chico Creek, Butte Creek, Clear Creek, and Dry Creek) with dependent variables including total metal concentrations, total major cation concentrations, sulfate, nitrate, and DOC, and independent variables including percent urban land use in watershed, number of burned structures per watershed, TSS, and flow as measured in Butte Creek. Each point represents a discrete sampling event, and shaded areas confine discrete samples within each watershed. RDA was plotted using the scaling I method (correlation biplot).